Earthquake Research Advances 5 (2025) 100349

Contents lists available at ScienceDirect

Earthquake Research Advances

journal homepage: www.keaipublishing.com/en/journals/earthquake-research-advances

Physical mechanisms of earthquake nucleation and foreshocks: Cascade triggering, aseismic slip, or fluid flows?

Zhigang Peng [a,*], Xinglin Lei [b,c]

[a] School of Earth and Atmospheric Sciences Georgia Institute of Technology, Atlanta, GA, 30332, United States
[b] Geological Survey of Japan, National Institute of Advanced Industrial Science and Technology, Ibaraki, 305-8567, Japan
[c] Now at State Key Laboratory of Earthquake Dynamics, Institute of Geology, CEA, Beijing, China

ARTICLE INFO

Keywords:
Foreshocks
Earthquake swarms
2024 Noto earthquake
Earthquake nucleation
Fluids
Aseismic slip
Haicheng earthquake

ABSTRACT

Earthquakes are caused by the rapid slip along seismogenic faults. Whether large or small, there is inevitably a certain nucleation process involved before the dynamic rupture. At the same time, significant foreshock activity has been observed before some but not all large earthquakes. Understanding the nucleation process and foreshocks of earthquakes, especially large damaging ones, is crucial for accurate earthquake prediction and seismic hazard mitigation. The physical mechanism of earthquake nucleation and foreshock generation is still in debate. While the earthquake nucleation process is present in laboratory experiments and numerical simulations, it is difficult to observe such a process directly in the field. In addition, it is currently impossible to effectively distinguish foreshocks from ordinary earthquake sequences. In this article, we first summarize foreshock observations in the last decades and attempt to classify them into different types based on their temporal behaviors. Next, we present different mechanisms for earthquake nucleation and foreshocks that have been proposed so far. These physical models can be largely grouped into the following three categories: elastic stress triggering, aseismic slip, and fluid flows. We also review several recent studies of foreshock sequences before moderate to large earthquakes around the world, focusing on how different results/conclusions can be made by different datasets/methods. Finally, we offer some suggestions on how to move forward on the research topic of earthquake nucleation and foreshock mechanisms and their governing factors.

1. Introduction

Most earthquakes are caused by the rapid dynamic rupture along pre-existing fault planes (Cocco et al., 2023; Scholz, 2019). Recent studies have found a wide range of fault slip behaviors, ranging from steady creep, slow earthquakes (i.e., aseismic fault slip, and deep tremor and low-frequency earthquakes) and regular earthquake ruptures (Peng and Gomberg, 2010; Avouac, 2015; Harris, 2017; Bürgmann, 2018; He et al., 2023; Ide and Beroza, 2023). However, laboratory experiments and numerical simulations on relatively homogeneous faults show that unstable fault slip is preceded by a development process (i.e., nucleation) from static to dynamic including a preslip phase (Ohnaka and Shen, 1999; Okubo and Dieterich, 1984; Dieterich, 1992; Ohnaka, 1992, 2013; Ampuero and Rubin, 2008). Here we define **preslip** as the aseismic slip that precedes the irreversible dynamic fault rupture. Laboratory experiments (Lei and Ma, 2014; McLaskey, 2019; Yamashita et al., 2021; Goebel et al., 2024) and numerical studies (Cattania and Segall, 2021; He et al., 2023) have shown that this process can greatly vary in time and space scales depending on factors such as the uniformity of the fault geometry and frictional property. Other recent studies also suggest that geometric complexities, frictional properties and fault orientations with respect to the maximum ambient stress directions play important roles in determining the fault slip mode of individual earthquakes, their collective behaviors, and nucleation processes before large earthquakes (Ben-Zion, 2008; Gabriel et al., 2024; Lee et al., 2024).

Foreshocks are a group of small to moderate-size earthquakes

* Corresponding author.
E-mail address: zpeng@gatech.edu (Z. Peng).

Production and Hosting by Elsevier on behalf of KeAi

https://doi.org/10.1016/j.eqrea.2024.100349
Received 27 August 2024; Received in revised form 7 November 2024; Accepted 10 November 2024

occurring in a relatively short space-time window before a larger earthquake (i.e., the **mainshock**) (Mogi, 1963). Strictly speaking, there should be a physical or statistically significant causal relationship between true foreshocks and the mainshock, and foreshocks should be clearly distinguished from the ordinary background activity. Otherwise, the term **preshocks** (Kanamori, 1981) are more appropriate for this definition. So far foreshocks can only be defined after the occurrence of the **mainshock** (i.e., the largest event in a sequence). For example, about 1/3 to 1/2 of the large mainshocks have foreshocks (Reasenberg, 1999; Chen and Shearer, 2016). But this number depends strongly on which earthquake catalogs are used, and how foreshock sequences are defined or identified (Trugman and Ross, 2019; van den Ende and Ampuero, 2020; Moutote et al., 2021). On the other hand, only 5–10% of small-size earthquakes are followed within one week of a larger magnitude event (Reasenberg, 1999; Christophersen and Smith, 2008). The successful short-term earthquake forecast for the 1975 M_S7.3 Haicheng earthquake in northeast China (Wang et al., 2006; Chen and Wang, 2010) was primarily based on observed foreshock swarm initiated two days before the earthquake. However, there were many similar swarms observed in the Chinese mainland, which were not followed by larger earthquakes (Chen et al., 1999; Lei et al., 2024). In addition, while some studies have argued that the statistical behaviors (i.e., the triggering productivity and the magnitude-frequency distributions or b-values) for foreshocks are different from other sequences (e.g., Lin, 2009; Gulia and Wiemer, 2019; Ito and Kaneko, 2023), other studies have shown virtually no difference between them (Felzer et al., 2004, 2015), or the signal is too subtle to be of any practical use (Dascher-Cousineau et al., 2020; van der Elst, 2021). These studies highlight the challenges to discriminate foreshocks from other earthquake sequences (Ogata et al., 1996) and use them as a reliable precursor for upcoming large earthquake (Zaccagnino et al., 2024). In this paper, the term "**earthquake precursor**" refers to a specific concept: it describes phenomena occurring near the epicenter before a major earthquake that can be reasonably explained based on current understanding and are intrinsically linked to the nucleation process of the earthquake.

An alternative approach is to estimate the probability of near-future earthquakes based on the past and current seismic activity and statistical forecasting models, such as the Epidemic Type Aftershock-Sequences (ETAS) model (Ogata, 1988). The ETAS model uses the established relationship in statistical seismology (Utsu et al., 1995; Utsu, 2002) such as the Omori's law for aftershock decay (Omori, 1894) and the Gutenberg-Richter (G-R) magnitude-frequency relationship (Gutenberg and Richter, 1944). These empirical relationships have been widely used to forecast large aftershocks after a major event (Ogata, 2017; Hardebeck et al., 2024; Mizrahi et al., 2024), or twin ruptures (i.e., two earthquakes of similar sizes) (Fukushima et al., 2023). They are also the theoretic basis of **operational earthquake forecasting (OEF)** (Jordan et al., 2011, 2014), with the goal of providing authoritative information about the changing seismic hazard during an earthquake sequence to help communities prepare for future earthquakes. Although OEF has been in places at several countries (e.g., Italy) (Spassiani et al., 2023), there were ongoing debates on whether the short-term changes in the seismicity rate justifies a public announcement for promoting seismic safety (Jordan and Jones, 2010; Jordan et al., 2011, 2014; Goltz, 2015; Wang and Rogers, 2014, 2017). The most recent example of OEF is the 'megaquake advisory' along the Nankai trough in southwest Japan issued by Japan Meteorological Agency (JMA) following a magnitude 7.1 earthquake off the coast of Kyushu Island in southwest Japan on August 8, 2024 (Toda et al., 2024). However, its ability to accurately forecast future large mainshocks is likely limited, given the fact that most triggered earthquakes are aftershocks that are smaller than the parent triggering event, and only a very small percentage of them are larger than the triggering event (i.e., foreshocks).

In this article, we provide a review of precursory signals before large earthquakes, focusing primarily on seismic (i.e., foreshocks) and aseismic slip behaviors, and various physical mechanisms that have been proposed so far for earthquake nucleation. We highlight primary differences in the results from several well-studied foreshock sequences and offer possible explanations. We do not provide a comprehensive review of other types of precursory signals, but instead refer the readers to the following papers on earthquake prediction (Kanamori, 2003), aseismic deformation before large earthquakes (Roeloffs, 2006), radon gases (Riggio and Santulin, 2015) and other geochemical precursors (Huang et al., 2017; Lu et al., 2023), laboratory acoustic emissions (Lei and Ma, 2014), earthquake nucleation (Ohnaka, 2013), seismo-electromagnetic precursors (Uyeda et al., 2009; Freund, 2011; Chen et al., 2022), foreshocks and mainshock nucleation (Ellsworth, 2019; Kato and Ben-Zion, 2021; He et al., 2023; Martínez-Garzón and Poli, 2024), and insights gained from injection-induced earthquakes (Lei et al., 2020; Ge and Saar, 2022; Moein et al., 2023). Finally, and most importantly, we point out potential future directions, focusing on physical mechanisms of earthquake nucleation and foreshocks and their governing factors in order to find answers to the following key questions: 1) What are the debates of foreshock identification, and with progresses in the technologies, can we be more precise in defining foreshocks? 2) What factors control the time, space, and amplitude difference between the foreshocks and/or preslip signals and the subsequent mainshock? 3) Whether the preslip signals are more evident when the mainshock is bigger? 4) How can we understand and utilize the interaction between fast and slow fault movement and fluid flow?

2. Foreshocks and other precursory signals

There is a long history of both failed attempts and a few limited successes in studying earthquake precursors and earthquake prediction (Bakun et al., 2005; Roeloffs, 2006; Wang et al., 2006; Ouzounov et al., 2018). For example, the aforementioned 1975 M_S 7.3 Haicheng earthquake was preceded by a swarm of foreshocks that occurred on the conjugate faults in the extensional step-over zone in the middle of the main rupture fault and lasted for about two days (Jones et al., 1982; Chen et al., 1999; Lei et al., 2024). While there is still some argument on whether the Haicheng earthquake prediction was considered as a true success or not, the foreshock sequence was one of the most important precursors (Wang et al., 2006; Chen and Wang, 2010). In any case, this is the only instance so far where the government issued an earthquake prediction and evacuation mobilization, significantly reducing casualties from the subsequent mainshock. As the year 2025 being the 50-year anniversary of the Haicheng earthquake prediction, it is important to revisit what progress has been made in the past half century on our understanding of foreshocks, earthquake nucleation and precursory signals.

Partially motivated by the apparent success of the Haicheng earthquake prediction, and the development of plate tectonics and rock dilatancy theory (Scholz et al., 1973) in the early 1970s, there was a heightened sense of optimism that reliable earthquake precursors existed, and earthquake prediction was just around the corner. However, the results from efforts in subsequent decades were mostly negative. For example, the 1995 M_W 6.8 (M_S 7.3) Menglian earthquake that occurred near the border between China and Myanmar was predicted, based primarily on the intensive foreshocks and other precursory anomalies (Li, 1996; Silver and Wakita, 1996; Chen et al., 1997; Lin, 2003). Based on the apparent 22-year recurrence of similar M6-type earthquake along the Parkfield section of the San Andreas Fault in Central California and their similar characteristics, including the famous 17-min M5 foreshock before the 1934 and 1966 Parkfield mainshocks (Bakun and McEvilly, 1979), the Parkfield earthquake prediction experiment was proposed (Bakun and Lindh, 1985), with the expected event between 1988 and 1993. The long-waited M 6 Parkfield earthquake did occur in 2004, arguably the most well recorded event around the world at that time. However, it was not preceded by any observable precursors (Langbein et al., 2005; Bakun et al., 2005). Instead, this event apparently initiated at the other side of fault segment that was broken during the 1934 and the 1996 M 6 Parkfield earthquake, and no observable foreshocks occurred within the last

few days near the epicentral region (Langbein et al., 2005; Neves et al., 2023). However, detailed analysis of deep tectonic tremor and low-frequency earthquakes indicated an increase of tremor activity and migration patterns in the last few months of the Parkfield mainshock, likely indicating aseismic slip in the lower crust beneath the nucleation zone of the 2004 *M* 6.0 mainshock (Nadeau and Guilhem, 2009; Shelly, 2009). This sequence, along with other studies during early 2000s (Roeloffs, 2006), highlighted the difficulty in detecting reliable precursors for short-term earthquake prediction.

Nevertheless, there is a renewed interest in studying earthquake precursory phenomenon in the last few years (Pritchard et al., 2020), largely driven by improved observations from both near-field (including off-shore) seismic and geodetic recordings (Ben-Zion et al., 2022), availability of big data in seismology (Arrowsmith et al., 2022), and promises in artificial intelligence (AI)/Machine Learning (ML) methods in seismology (Beroza et al., 2021; Mousavi and Beroza, 2023) and other scientific domains (Wang et al., 2023). Using spatio-temporal changes in background seismicity and continuous GNSS recordings, recent studies have found clear anomalies up to several years for earthquakes in Japan (Ogata, 2005, 2007). A recent analysis of high-rate GNSS time series also found a 2-h-long exponential acceleration of aseismic slip before 90 $M_W > 7$ earthquakes around the globe (Bletery and Nocquet, 2023, 2025), and a ML method was applied to identify potential precursory patterns in small earthquakes before two large *M* 7+ earthquakes in California and Alaska (Girona and Drymoni, 2024). However, these results were challenged by subsequent re-analysis (Bradley and Hubbard, 2023, 2024a, 2024b). Similarly, migrating foreshocks, repeating earthquakes (Kato et al., 2012) and offshore geodetic observations (Ito et al., 2013) all suggested the existence of slow slip before the 2011 *M* 9 Tohoku-Oki earthquake along the Japan subduction zone. However, stacked tiltmeter records did not show accelerating-like deformation starting 2 hr before the mainshock (Hirose et al., 2024), suggesting that such aseismic slip, if exists, would be less than a moment magnitude M_W 6.4 earthquake. In addition, it cannot be determined whether it links to the preslip of the mainshock. On the other hand, migratory aseismic slip and abundant foreshocks are frequently observed for daily ice stream earthquakes at the Whillans Ice Plain, West Antarctica (Barcheck et al., 2021). The month-long swarm-like foreshocks before the 2014 *M* 8.2 Iquique earthquake sequence in Northern Chile was also likely driven by geodetically observable slow-slip events, likely reflecting the preslip of the mainshock (Ruiz et al., 2014; Schurr et al., 2014). However, Bedford et al. (2015) argued that most observed aseismic transients can be attributed to post-seismic slip following moderate-size earthquakes (i.e., **afterslip**) in the last 1–2 months before the Iquique mainshock. More recently, Twardzik et al. (2022) found that a slow slip event is needed to explain most of the geodetic observation, but it did not behave like a self-accelerating slip event. Instead, it interacted with the moderate-size foreshock sequence.

In addition to subduction zone settings, aseismic slip or fluid migration have been invoked to as the primary physical mechanisms driving the foreshock sequence along oceanic transform faults (McGuire et al., 2005; Liu et al., 2020) and continental settings (Zhou et al., 2022; Wang et al., 2024a; Lei et al., 2024). More recently, both aseismic slip and elevated fluids are found to work in concert to drive a prolonged earthquake swarm that started beneath the Noto Peninsula in Central Japan since November 2020 (Amezawa et al., 2023; Kato, 2024; Nishimura et al., 2023; Yoshida et al., 2023a, 2023b, 2024), which culminated in the 2024 *M* 7.5 Noto mainshock (Toda and Stein, 2024; Ishikawa and Bai, 2024). The Noto Peninsula mainshock was preceded by three immediate foreshocks in the magnitude ranges of *M* 5-6 in the last 4, 2 min and 14 s before, likely reflecting a change from the long-term swarm-like behavior to a burst-like foreshock sequence (Peng et al., 2025). Geochemical analysis in the Noto epicentral region also indicated that the fluid sources are likely from upper mantle (Umeda et al., 2024). Similarly, several studies also found possible evidence of prolonged preparation processes before the 2023 *M* 7.8 Pazarcik, Türkiye earthquake (Picozzi et al., 2023; Kwiatek et al., 2023), although no immediate foreshocks were identified.

In summary, while in some cases aseismic process or fluid flows have been observed before large earthquakes (e.g., the 2014 *M* 8.2 Iquique and the 2024 *M* 7.5 Noto Peninsula sequences), these processes are not clearly present in other well studied cases (i.e., the 2004 *M* 6 Parkfield earthquake), highlighting again the challenge of identifying a reliable precursory signal before moderate to large earthquakes. Here, understanding the dominant factors that cause such differences is a crucial task to answer questions raised in the Introduction section.

3. Foreshock types

Mogi (1985) attempted to define foreshocks of two types. In the first type (type C in his definition), seismic activity gradually increases toward the mainshock. In the second type (type D in his definition), the increasing foreshock activity dies down before the occurrence of the mainshock. However, foreshock observations in the past few decades suggest a much more complex patterns than those two types (Martínez-Garzón and Poli, 2024). Based on their temporal behaviors, here we attempt to classify foreshock behaviors into the following types: no immediate foreshocks/quiescence, accelerating, burst, swarm and two hybrid types (Fig. 1). Table 1 also lists these types and the corresponding example sequences.

Sometimes large earthquakes occur without obvious foreshocks and show an apparent quiescence in the last few days/weeks preceding the mainshock (Fig. 1a). For example, while there were some increases of seismic activity and slow slip derived from repeating earthquakes in a broader region starting a few years to a few months before, there were no immediate foreshocks (i.e., in the last few days) before the 2008 *M* 7.9 Wenchuan, China earthquake (Chen and Wang, 2010; Li et al., 2011; Ruan et al., 2017) and the 2023 *M* 7.8 Pazarcik, Türkiye, earthquake, the first mainshock of the Kahramanmaraş sequence (Kwiatek et al., 2023; Picozzi et al., 2023).

The *accelerating-type* foreshocks (Fig. 1b) are mostly found in laboratory settings as acoustic emissions (Lei and Ma, 2014; McLaskey, 2019; Yamashita et al., 2021; Bolton et al., 2023; Goebel et al., 2024; Lei, 2024). In natural setting, except in a few cases (e.g., Bouchon et al., 2011) or for stacked sequences (Maeda, 1999; Bouchon et al., 2013; Felzer et al., 2015; Shearer et al., 2023), most foreshocks do not show clear accelerating patterns before the mainshock.

In the *burst-type* (Fig. 1c), a moderate-size foreshock would be followed by its own aftershocks that decays with time, and then the larger mainshock happens. Examples include the 1995 *M* 6.0 (M_S 7.3) Menglian, China earthquake (Chen et al., 1997, 1999; Lin, 2003), 2010 *M* 6.7 Yushu, China earthquake (Ni et al., 2010; Chuang et al., 2023; Huang et al., 2023), the 2014 *M* 7.3 Yutian, China earthquake (Li et al., 2024a), the 2016 *M* 7.0 Kumamoto, Japan earthquake (Kato et al., 2016; Yue et al., 2017) and the 2019 *M* 7.1 Ridgecrest, California earthquake (Ross et al., 2019b; Wang et al., 2020; Huang et al., 2020; Yue et al., 2021). The time scale between the moderate-size foreshock and the larger mainshock varies but is typically in the range of days to weeks. Sometimes the magnitude of the largest foreshock and the mainshock is relatively small (i.e., less than 0.5). In this case, it can also be classified as doublet sequence. Examples include the 1976-05-29 M_S 7.4 Longling, China sequence (Zuo et al., 1996), and the 1987 Superstition Hill earthquake sequence (Hudnut et al., 1989).

In the *swarm-type* (Fig. 1d), the mainshock is preceded by an earthquake swarm without a clear dominant event or there are some events with progressively increase of magnitude before the largest foreshock (i.e., opposite of the third burst-type). Examples of this type include the 1966 *M* 6.8 Xingtai, China earthquake (Chung and Cipar, 1983; Chen et al., 1999), 1975 *M* 7.0 (M_S 7.3) Haicheng earthquake (Jones et al., 1982; Chen et al., 1999; Wang et al., 2006; Lei et al., 2024) and the 2010 *M* 7.2, El-Mayor Cuccapah earthquake (Hauksson et al., 2011; Yao et al., 2020).

In the *first hybrid-type* (Fig. 1e), the foreshock activity typically starts

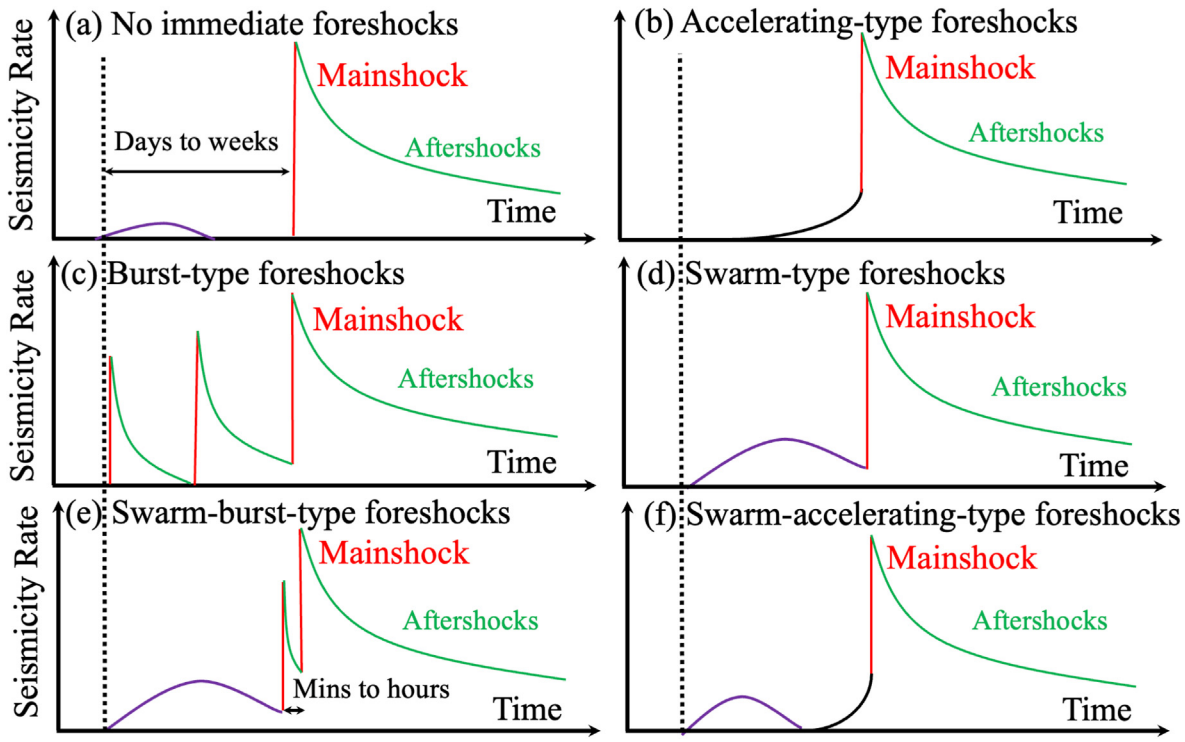

Fig. 1. Schematic diagrams showing temporal behaviors of different types of foreshock sequences. In each plot, the purple color denotes swarms or accelerating foreshocks, the red color denotes the mainshock and large foreshocks, and green color denotes aftershocks of the mainshock and large foreshocks. (a) No obvious foreshocks right before the mainshock; (b) Accelerating-type foreshocks where the seismicity rate increases exponentially before the mainshock; (c) Burst-type foreshocks where each moderate-size foreshocks are followed by their own aftershocks; (d) Swarm-type foreshocks where the foreshock sequence can be classified as a swarm; (e) Swarm-burst-type foreshocks where the sequence include a swarm and a subsequent moderate-size event (and its aftershocks) right before the mainshock; (f) Swarm-accelerating-type foreshocks where the foreshock sequence starts as an swarm, a subsequent quiescence, and finally an accelerating sequence right before the mainshock.

with a swarm-type sequence that can last weeks or months. Right before the mainshock, there is clear change of the behaviors from swarm-type to burst-type, which would include one or a few moderate-size foreshocks with their own aftershocks, and the mainshock itself. Examples of this type include the 2009 M 6.1 L'Aquila earthquake (Valoroso et al., 2013; Sugan et al., 2014; Vuan et al., 2018; Cabrera et al., 2022), the 2011 M 9.1 Tohoku-Oki earthquake (Hirose et al., 2011; Kato et al., 2012), the 2014 M 8.2 Iquique earthquake (Ruiz et al., 2014; Schurr et al., 2014; Kato and Nakagawa, 2014; Meng et al., 2015), the 2018 M 6.8 Zakynthos earthquake along the Hellenic subduction zone (Papadopoulos et al., 2020), and the 2021 M 6.1 Yangbi earthquake (Lei et al., 2021; Zhou et al., 2022; Zhu et al., 2022a; Liu et al., 2022; Wang et al., 2024a).

In the *second hybrid-type* (Fig. 1f), a mainshock was preceded by a swarm-like sequence a few months or years before the eventual mainshock, followed by an apparent quiescence, and then accelerating-type foreshocks occurred right before the mainshock. A well-known example is the 1923 M 7.9 Great Kanto earthquake sequence in Japan (Ohnaka, 1984; Ohnaka, 2013). However, Suyehiro and Sekiya (1972) showed that no immediate foreshocks were identified right before the Kanto mainshock. Depending on how the last 4 min of the foreshock activity is classified, especially whether the last foreshock of M 5.9 occurring ~14 s before the mainshock is considered as an individual event or part of the mainshock nucleation (Ma et al., 2024; Xu et al., 2024b), the foreshock sequence of the 2024 M 7.5 Noto Peninsula earthquake can be viewed as either of the two hybrid types (Shelly, 2024; Peng et al., 2025; Toda and Stein, 2024; Yoshida et al., 2024).

We note that the above classification is not strict or mutually exclusive. Besides the two hybrid types, transitional types may also occur. For example, the entire foreshock sequence of the 2021 M 6.1 Yangbi earthquake can be viewed as the swarm-type. However, it includes three episodes, and the first two started with moderate-size earthquakes followed by their own aftershocks (Lei et al., 2021; Zhu et al., 2022a; Zhou et al., 2022). The last episode started with a M 4.1 earthquake in the last 1 h, and the largest foreshock of M 5.1 occurred in the last 30 min before the mainshock. Hence, it can also be classified as the first hybrid type. Additionally, depending on the inspected time windows, we would end up with different types. For example, while the overall foreshock behavior of the foreshock for the 2010 M 7.2 El-Mayor Cuccapah mainshock (Hauksson et al., 2011; Yao et al., 2020) was swarm-like, if we zoom in in the last day and especially in the last hours, there were several $M > 3$ earthquakes in the last 6 min of the 2010 M 7.2 El-Mayor Cuccapah mainshock (Yao et al., 2020), which clearly did not follow the overall swarm-type behaviors in the last two days. In this case, it would likely be classified as one of the hybrid-type, rather than the swarm-type. Again, it is an important issue to understand the governing factors behind each foreshock type.

4. Physical mechanisms of foreshocks

One motivation for such classification for foreshocks is that it may reflect differences in their driving mechanisms and structures within the source region. In general, each burst in the burst-type foreshocks (Fig. 1c) behaves like a mainshock-aftershock sequence, and the total foreshocks could be simply modeled by statistical processes such as the Omori's law for aftershock decay (Utsu et al., 1995; Utsu, 2002; Kanamori and Brodsky, 2004) or the ETAS model, which encompasses both the Omori law and the G-R law of magnitude-frequency distribution (Ogata, 1988, 2017). Their similar behaviors to aftershock sequence also suggest a similar physical mechanism for both foreshocks and aftershocks. On the other hand, swarm-like behaviors can also be modeled using ETAS but requires considering external driving factors that may vary over time (Petrillo et al., 2024), such as episodic fluid flow or slow-slip events,

Table 1
List of Different Foreshock Types, Example Earthquake Sequences and References

Foreshock Types	Example Mainshocks	The Largest Foreshock	Foreshock Durations	Other Precursory/Unique Observations	References
(a) no foreshocks	• 2004-09-28 *M* 6.0 Parkfield, California earthquake	• n/a	• n/a	• Changes in tremor activities ~3 months before	• Langbein et al. (2005); Bakun et al. (2005); Shelly (2009); Nadeau and Guilhem (2009); Neves et al. (2023)
	• 2008-05-12 *M* 7.9 Wenchuan, China earthquake	• n/a	• n/a	• A swarm sequence ~88 days before not in the epicenter region	• Chen and Wang (2010); Li et al. (2011); Ruan et al. (2017)
	• 2023-02-06 *M* 7.8 *M* 7.8 Pazarcik, Türkiye earthquake	• n/a	• n/a	• A seismicity transient 8 months before	• Kwiatek et al. (2023); Picozzi et al. (2023)
(b) Accelerating-type foreshocks	• 1999-08-17 *M* 7.6 İzmit, Türkiye earthquake	• *M* 2.9	• 44 min	• Nearly repeating earthquakes	• Bouchon et al. (2011); Ellsworth and Bulut (2018)
	• Stacked foreshocks	• n/a	• n/a	• n/a	• Maeda (1999); Bouchon et al. (2013); Felzer et al. (2015); Shearer et al. (2023)
	• Laboratory experiments	• n/a	• n/a	• Aseismic slip, changing b values, changing seismic velocities	• Lei & Ma (2014); McLaskey (2019); Yamashita et al. (2021); Bolton et al. (2023); Goebel et al. (2024); Lei (2024)
(c) Burst-type foreshocks	• 1976-05-29 M_S7.4 Longling, China earthquake	• M_S7.3	• ~123 min (~97 min, the largest foreshock)	• A doublet sequence	• Zuo et al, (1996)
	• 1987-11-24 *M* 6.5 Superstition Hill, CA earthquake	• *M* 6.0	• 11.4 hr	• Conjugate faults	• Hudnut et al. (1989)
	• 1995-07-12 *M* 6.8 (M_S7.3) Menglian, China earthquake	• *M* 6.2	• < 30 hr	• Prediction issued	• Chen et al. (1997, 1999); Lin (2003)
	• 2010-04-11 *M* 6.7 (M_S7.3) Yushu, China earthquake	• *M* 4.6	• 130 min	• Conjugate faults	• Ni et al. (2010); Chuang et al. (2023); Huang et al. (2023)
	• 2014-02-12 *M* 6.9 (M_S7.3) Yutian, China earthquake	• M_S5.4	• ~31 hr	• n/a	• Li et al. (2024)
	• 2016-04-15 *M* 7.0 (*Mj*7.3) Kumamoto, Japan earthquake	• *M* 6.2 (*Mj* 6.5)	• ~28 hr	• Migrating foreshocks, low b value	• Kato et al. (2016); Yue et al. (2017)
	• 2019-07-06 *M* 7.1 Ridgecrest, U.S. earthquake	• *M* 6.4	• ~34 hr	• Repeating/migrating foreshocks, Geodetic transients	• Ross et al. (2019b); Wang et al. (2020); Huang et al. (2020); Yue et al. (2021)
	• 1966-03-22 *M* 6.8 Xingtai, China earthquake	• *M* 6.2	• ~15 days	• Multiple foreshocks and aftershocks with M>6	• Chung and Cipar (1981); Chen et al. (1999)
(d) Swarm-type foreshocks	• 1975-02-02 *M* 7.0 (M_S7.3) Haicheng, China earthquake	• M_S5.2	~4 days (~12 hr, the largest foreshock)	• Migrating foreshocks, Conjugate faults; Prediction issued	• Jones et al. (1982); Chen et al. (1999); Wang et al. (2006); Lei et al. (2024)
	• 2010-04-04 *M* 7.2 El-Mayor Cuccapah, Mexico earthquake	• *M* 4.2 (M_L4.4)	• ~21 days (~24 hr, the largest foreshock)	• Migrating foreshocks, Conjugate faults	• Hauksson et al. (2011); Yao et al. (2020)
	• 2009-04-06 *M* 6.1 L'Aquila, Italy earthquake	• *M* 4.0	• ~ 4 months (~ 1-week, the largest foreshock)	• Different seismicity behaviors, evidence for aseismic process	• Valoroso et al. (2013); Sugan et al. (2014); Vuan et al. (2018); Cabrera et al. (2022)
(e) Swarm-burst-type foreshocks	• 2011-03-11 *M* 9.0 Tohoku-Oki, Japan earthquake	• *M* 7.3	• ~23 days (2 day, the largest foreshock)	• Different migrating patterns, aseismic events in questions	• Hirose et al. (2011); Kato et al. (2012); Ito et al. (2013); Hirose et al. (2024)
	• 2014-04-04 *M* 8.2 Iquique, Chile earthquake	• *M* 6.7	• ~17 days (~16 day, the largest foreshock)	• Migrating foreshocks, evidence for slow slip	• Ruiz et al. (2014); Schurr et al. (2014); Kato and Nakagawa (2014); Meng et al. (2015); Bedford et al. (2015);
	• 2018 *M* 6.8 Zakynthos earthquake along the Hellenic subduction zone ()	• *M* 4.8	• ~ 6 months (50 min, the largest foreshock)	• Multiple stages of foreshock swarms, b-value change	• Twardzik et al. (2022); Papadopoulos et al., 2020
	• 2021-05-21 *M* 6.1 Yangbi, China earthquake	• *M* 5.1	• ~3 days (30 min, the largest foreshock)	• Multiple episodes of foreshocks, repeating earthquakes, aseismic slip in the last hour	• Lei et al. (2021); Zhou et al., 2022; Zhu et al. (2022); Liu et al. (2022); Wang et al. (2024a)
	• 1923-09-01 *M* 7.9 Great Kanto, Japan earthquake	• n/a	• ~3 years (no immediate foreshocks)	• Changes in crustal deformation, during a dry typhoon	• Suyehiro and Sekiya (1972); Ohnaka (1984, 2013)
(f) Swarm-accelerating-type foreshocks	• 2024-01-01 *M* 7.5 Noto Peninsula, Japan earthquake	• *M* 5.9	• ~3-year swarm (4 min immediate foreshocks;14 s, the largest foreshock)	• Migrating swarm, aseismic slip, slow initial mainshock rupture	• Kato (2024); Ma et al. (2024); Peng et al. (2025); Shelly (2024); Toda and Stein (2024); Yoshida et al. (2024); Xu et al. (2024b)
Foreshock Types	**Example Mainshocks**	**The Largest Foreshock**	**Foreshock Durations**	**Other Precursory/Unique Observations**	**References**

within the background seismic activity (Vidale and Shearer, 2006). Similar approaches have been successively applied to injection-induced seismic activities to account the role of injection operations (e.g., Lei et al., 2019; Lei et al., 2020; Jia et al., 2020; Moein et al., 2023).

Fig. 2 summarize five physical models of earthquake nucleation and foreshocks that have been proposed so far. The first three models are presented in McLaskey (2019), while the last two are from two recent studies (Lei et al., 2024; Wang et al., 2024a). The *preslip* model (Fig. 2a) asserts that precursory aseismic slip occurs during earthquake nucleation, which can drive both foreshocks as well as the initial rupture of the mainshock (Dieterich, 1992; Ohnaka, 1992, 2013; Dodge et al., 1996; Bouchon et al., 2011; He et al., 2023). In this case, the size of a critical length scale *Lc* before the onset of the dynamic rupture is likely on the order of kilometer scales and is capable of hosting both aseismic slip and foreshocks (McLaskey, 2019; Wu and McLaskey, 2022). The *cascade* or *cascade triggering* model (Fig. 2b), on the other hand, describes that both foreshocks and the mainshock initiation as a random process that are linked by elastic stress triggering (Ellsworth and Bulut, 2018). In other words, a mainshock is considered as an event triggered by the preceding earthquake which happens to be larger (Helmstetter et al., 2003; Felzer et al., 2004). In this case, the critical length scale *Lc* is on the meter scale, indicating that small and large earthquakes nucleate in the same fashion (Ide, 2019; Münchmeyer et al., 2022) and elastic stress transfer (i.e., the *cascade* model) would likely dominate in triggering each other (including the mainshock). Martínez-Garzón and Poli (2024) argues that both *preslip* and *cascade* models are likely end-member models that may oversimplify the real processes. Mignan (2014) found that studies with smaller events listed in the earthquake catalogs favored more on the *preslip* model, suggesting a potential bias due to catalog completeness. In the *rate-dependent cascade-up* model (Fig. 2c), the nucleation process includes *preslip* that can drive foreshocks, but the occurrence of foreshocks can trigger a rapid dynamic rupture of the mainshock (i.e., *cascade triggering*) (Noda et al., 2013; McLaskey and Lockner, 2014; McLaskey, 2019; Wu and McLaskey, 2022). McLaskey (2019) pointed out that the size of the critical length scale *Lc* played an important role in determining whether *preslip* or *cascade* model likely dominates in the earthquake nucleation process. Higher loading rates from large foreshocks can temporally reduce the critical length scale *Lc* (e.g., Guérin-Marthe et al., 2019; Kaneko and Lapusta, 2008), resulting in abrupt initiation of the mainshock (i.e., the *rate-dependent cascade-up* model).

In the *fluid-driven* model (Fig. 2d), episodic fluid flow (most likely from larger depth) is the primary driver for the foreshock activity as well as the initiation of the mainshock (Jansen et al., 2019; Lei et al., 2024). In this case, foreshock seismicity fronts expand from the initial injection point (if the fluid source can be approximated as a point) with sqrt(*t*) (Shapiro et al., 1997), and likely cover a much wider area than the critical nucleation length scale *Lc* of the mainshock. In the *migratory slow-slip* model (Fig. 2e), aseismic slip, rather than fluid flow, is hypothesized to be the main driver of the foreshock and the mainshock initiation (Barcheck et al., 2021; Wang et al., 2024a, 2024c). A major difference between this (Fig. 2e) and the *preslip* models (Fig. 2a) is that the aseismic slip area here is much larger than the critical nucleation length scale *Lc* for dynamic slip of the subsequent mainshock. A recent study by Li et al. (2024b) suggests that the wavelength of normal stress variation λ with respect to the local critical nucleation length scale *Lc** controls the selection of nucleation models, and *migratory slow-slip* model could emerge when λ lies between *Lc** for high normal stress patch and that for low normal stress patch. Moreover, Moutote et al. (2023) argue that the same aseismic process not only drive the foreshock and mainshock nucleation, but also aftershock migration.

We note that these five models are the most representative ones, but other competing models have also been introduced. For example, Kato and Ben-Zion (2021) introduced a *progressive localization* model that involves an evolution of deformation from distributed damage in a rock volume to more localized shear slip along future rupture zones. During such localization process, elevated seismicity would occur in multiple clusters, and one of them would evolve into a foreshock sequence and finally initiate the mainshock. Possible examples include the 2014 M8.1 Iquique earthquake sequence in Northern Chile (Socquet et al., 2017), the 2016 Central Italy seismic sequence (Sugan et al., 2023), and likely the 2024 *M* 7.5 Noto Peninsula earthquake and preceding swarms (Kato, 2024; Peng et al., 2024). Such localization of deformation may occur in either geometrically simple or complex fault structures (Kato and Ben-Zion, 2021).

Based on numerical modeling of the nucleation process on homogenous fault that is governed by the rate-and-state friction law, He et al. (2023) found that a stress-releasing zone (termed weakening-zone core) expands first and then shrinks in the later stage right before the mainshock. They argued that the evolution of foreshock activity including its time-space migration before the 2014 M8.2 Iquique earthquake was consistent with such an expansion and shrinking pattern (Yagi et al., 2014). However, to reasonably explain both *preslip* and foreshocks, the "homogeneous" fault must contain some distributed asperities or sub faults. Just like what has been observed in the laboratory, before a

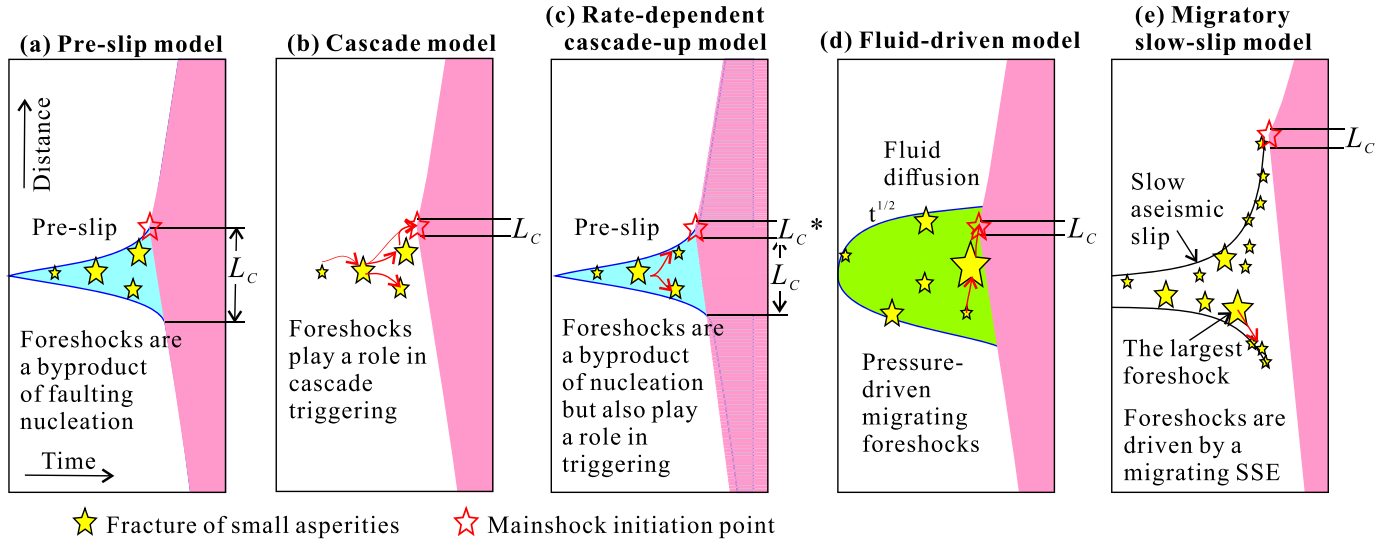

Fig. 2. Schematic diagrams showing five representative foreshock models that have been proposed so far. (a) Preslip; (b) Cascade; (c) Rate-dependent cascade-up; (d) Fluid-driven; and (d) Migratory slow-slip model. In each panel, Lc represents the critical nucleation length needed for the mainshock rupture to go unstable. Modified from McLaskey (2019) and Lei et al. (2024).

large-scale rupture occurs, the asperities within the nucleation zone of the fault need to break sequentially, forcing *preslip* to reach a critical scale (Lei, 2003). Finally, numerical modeling results suggest that *afterslip* (or more generally triggered aseismic slip) from previous earthquake can drive foreshocks and the next larger mainshock (Ito and Kaneko, 2023). Like the *cascade* model, their critical nucleation scale *Lc* can be much smaller than the region that hosts aseismic slip.

Recently, Stein and Bird (2024) proposed an alternative *cascade* model where large continental earthquakes (such as the 2023 *M* 7.8 Pazarcik, Türkiye, earthquake) likely nucleated on a branch or splay fault before jumping onto the major strike-slip fault (Fig. 3a). The initial rupture on the branch fault could be considered as a foreshock. However, depending on the time separation between the initial and the major ruptures, it can also be viewed as part of the mainshock rupture at teleseismic distances. For example, the 2024 *M* 7.5 Noto Peninsula mainshock was preceded by a *M* 5.9 foreshock 14 s earlier (Peng et al., 2024). But this event was only listed in the JMA catalog, not by the USGS or other global catalogs. Ma et al. (2024) showed that there was likely more than one event in these 14 s, and hence they argued for a continuous initial slow rupture, rather than one single foreshock (Fig. 3b). Ozacar and Beck (2004) also showed that the initial ruptures of the 2001 *M* 7.9 Kunlun fault and the 2002 *M* 7.9 Denali fault earthquakes all started on fault structures with different faulting styles than the main strike-slip faults (Fig. 3a). Regardless of the name of the branched fault rupture and its faulting style, it likely reflects an alternative view to consider how large ruptures on continental faults are initiated (Stein and Bird, 2024).

Finally, Martínez-Garzón and Poli (2024) reviewed several of these models and proposed an *integrated* model with the initial phase being the localization model, and the last stage being the *rate-dependent cascade-up* model. Similarly, based on precursory acoustic emission during nucleation of laboratory stick-slip experiment, Marty et al. (2023) argued that the nucleation process is almost entirely aseismic at the beginning, and is followed by increased proportion of elastic stress triggering right before the onset of mainshock rupture. This is similar to the *rate-dependent cascade-up* model (McLaskey, 2019).

Here we attempt to further classify these foreshock physical models into three categories: elastic stress changes, aseismic slip,and fluid flows (Fig. 4). Some physical models presented before (Fig. 3) can be combined into one category. For example, the *preslip* model (e.g., Dieterich, 1992; Ohnaka, 1992; Bouchon et al., 2011), the recently proposed *migratory*

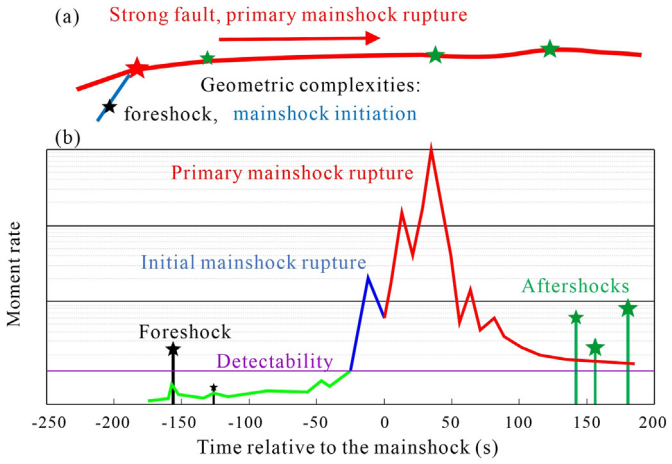

Fig. 3. (a) A schematic diagram showing a fault model where a large earthquake rupture on the main fault which is strong and is preceded by a foreshock. The initial mainshock rupture occurs on a subsidiary fault that has either a different fault orientation or different faulting style (Stein and Bird, 2024). The mainshock ruptures unilaterally to the right and is followed by numerous aftershocks. (b) A normalized moment rate function showing the initial and primary mainshock ruptures, which is preceded by a foreshock and followed by many aftershocks.

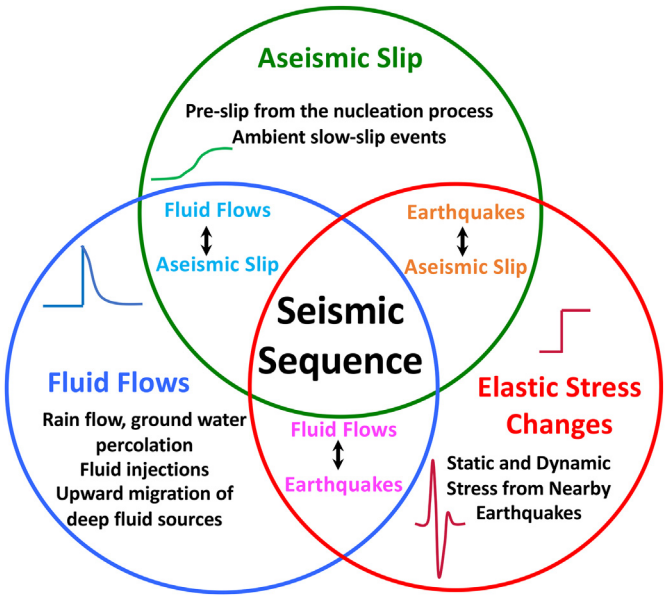

Fig. 4. An updated summary of three primary physical models that drive seismicity (foreshocks, aftershocks, swarms) and potential interactions between them.

slow-slip model (Barcheck et al., 2021; Wang et al., 2024a) and the *afterslip* model (Ito and Kaneko, 2023) can be all combined into the aseismic slip category. Similarly, the elastic stress change category would include both static and dynamic stress changes from nearby earthquake ruptures (i.e., the original and alternative cascade models), and possibly dynamic stress changes from nearby earthquake ruptures (Antonioli et al., 2006; Ding et al., 2023; Dong et al., 2024) and large distant earthquakes (Walter et al., 2015; Martínez-Garzón and Poli, 2024). It is also obvious that the physical process in each category is not mutually exclusive and can 'trigger' each other. For example, an earthquake can trigger aseismic slip surrounding the mainshock rupture plane, which is termed afterslip. Afterslip is known to drive aftershocks (Peng and Zhao, 2009; Ross et al., 2017; Perfettini et al., 2018; Itoh et al., 2023), and if the triggered aftershocks happen to be larger than the previous earthquake, we now have a case where afterslip (or more generally aseismic slip) from previous earthquake can drive foreshocks and the next larger mainshock (Ito and Kaneko, 2023). Similarly, based on the physical mechanisms of dilatancy hardening and fault slip affecting its hydraulic diffusivity, there are also interactions between fluid flows and slow preslip that can either promote or inhibit each other (Liu et al., 2020; Lei, 2024). Thus, while fluid flows can drive seismicity, the occurrence of moderate to large earthquakes are also known to break seals within the fault zones, resulting in rapid changes of fluid flows and subsequent seismicity through a fault-valve mechanism (Sibson, 2007; Kato, 2024). Finally, as mentioned before, aseismic slip and fluid flow can work in concert to drive foreshocks and earthquake swarms (Sirorattanakul et al., 2022; Peng et al., 2025).

We note that these models/categories have long been proposed to explain aftershocks or remotely triggered seismicity (Freed, 2005; Hill and Prejean, 2015; Hardebeck et al., 2024). Based on their statistical characteristics, some studies argue that we cannot tell foreshocks and aftershocks apart, until the largest mainshock occurs (Helmstetter et al., 2003; Felzer et al., 2004; Zaccagnino et al., 2024). When we observe seismic activity with characteristics like typical foreshocks known so far, determining whether it is a precursor to a major earthquake requires a comprehensive consideration of many factors, including the scale of local faults and their stress criticality and potential fluids. Despite decades of research progress, this still presents a challenging seismological issue.

5. Differences in foreshock observations and interpretations

In the past twenty years, several foreshock sequences have been well studied, although different conclusions were made on the physical mechanisms of mainshock nucleation and foreshock behaviors. Examples include the 1999 *M* 7.6 Izmit (Bouchon et al., 2011; Ellsworth and Bulut, 2018), the 2010 M6.7 Yushu earthquake (Chuang et al., 2023; Huang et al., 2023), the 2019 *M* 7.1 Ridgecrest earthquake (Ross et al., 2019b; Huang et al., 2020; Yue et al., 2021), and the 2021 *M* 6.1 Yangbi earthquake (e.g., Zhu et al., 2022a; Liu et al., 2022; Zhou et al., 2022; Wang et al., 2024a).

Below we attempt to highlight a few areas where majority of the differences reside. Fig. 5a shows the Coulomb stress changes from an *M* 4.6 foreshock that occurred more than 2 hr before the 2010 *M* 6.7 Yushu earthquake in the Tibetan Plateau in Western China (Chuang et al., 2023). The *M* 4.6 foreshock occurred on a conjugate fault plane and casted a negative Coulomb stress on the hypocenter of the *M* 6.7 mainshock. However, Huang et al. (2023) showed that while the *M* 4.6 foreshock occurred on the conjugate fault plane, both events were close to the same E-W trending Ganzi-Yushu fault. Such an alternative location would result in a small but positive Coulomb stress changes on the mainshock hypocenter, which is consistent with the *cascade* model. Similarly, Peng et al. (2024) found that an M5.5 foreshock occurred 4 min before the 2024 *M* 7.5 Noto Peninsula mainshock casted an apparent stress shadow (i.e., negative Coulomb stress change) at the mainshock hypocenter. Zhou et al. (2022) and Wang et al. (2024a) also found that by moving the hypocenter of the 2021 *M* 6.1 Yangbi mainshock from 4 km-5 km to 7 km–8 km depth, the Coulomb stress changes from preceding foreshocks on the Yangbi mainshock hypocenter became much smaller as compared to the previous results (Zhu et al., 2022a). Clearly, a change of relative location of a few kilometers between the foreshock and the mainshock can result in a significant change in the amplitude of the static Coulomb stress changes, sometimes even the sign. These comparisons highlight the need to compare different methods used to determine both the absolute and relative locations of the foreshock and the mainshock initial hypocenter. Besides event location, dynamic stress change could play a significant role. For example, the mainshock hypocenter could be first loaded by a positive dynamic Coulomb stress change and then a positive or negative static Coulomb stress change from a nearby foreshock (Antonioli et al., 2006; Ding et al., 2023; Dong et al., 2024). Slow slip or fluid flow may also generate stress changes at the mainshock hypocenter, but it is not generally considered when computing stress changes.

Repeating earthquakes (or repeaters) refer to a group of earthquakes occurring at essentially the same region, or more strictly speaking, correspond to the failure of the same asperity (Fig. 5b) and generating nearly identical waveforms (Vidale et al., 1994; Nadeau and McEvilly, 1999; Uchida, 2019). They are generally considered to be frictionally locked asperities surrounded by rate-strengthening region that either creep constantly, or slip during aseismic transient (Beeler et al., 2001; Uchida and Bürgmann, 2019; Nakajima and Hasegawa, 2023). Hence, their recurrence intervals and co-seismic slip can be used together to infer the amount of ambient aseismic slip or creep at depth (Nadeau and McEvilly, 1999; Materna et al., 2018; Deng et al., 2020; Nakajima and Hasegawa, 2023), preslip or aseismic slip before large earthquakes (Li et al., 2011; Kato et al., 2012; Chen and Li, 2018; He et al., 2023) or afterslip/postseismic deformation (Peng et al., 2005; Zhao and Peng, 2009; Chen et al., 2010; Yao et al., 2017). However, so far there is no universal criteria for defining repeating earthquakes. Depending on the threshold of the cross-correlation coefficient (CCC) and other parameters (e.g., time window length, frequency band), different groups may reach totally different conclusions on whether repeating earthquakes exist and their detailed clustering behaviors. Gao et al. (2021) recently pointed out that using CCC alone is not sufficient to distinguish between true tight repeaters (i.e., overlapping source regions) and loose repeaters (i.e., partially or close but non-overlapping source regions) (Fig. 4b). A combination of CCC and interevent overlapping region (based on relocations or differential S-P arrival times) is needed to identify those tight repeating clusters (Peng et al., 2005; Zhao and Peng, 2009; Gao et al., 2021; Sugan et al., 2022). Additionally, the mechanism of repeating earthquakes does not necessarily require aseismic slip (Ellsworth and Bulut, 2018). Laboratory studies have shown that continuous/cycled injection of fluid may also trigger repeated ruptures due to a decrease in the effective normal stress, as expected from the Mohr-Coulomb failure law (Zhu et al., 2021). In summary, inaccurate estimation of repeating earthquakes may lead to biased understanding of the physical process (aseismic slip or fluid flows) leading up to the mainshock.

Finally, different migration patterns of foreshocks have been used to infer different physical processes driving the sequence. Fig. 5c summarizes three types of seismicity migration curves and the corresponding driving forces. Steady slow-slip events (SSEs) tend to be followed by deep tectonic tremor at larger depth or microseismicity at shallower seismogenic depth (Kato, 2019; Wickham-Piotrowski et al., 2024), and the seismicity typically track the slip front of the SSEs. If the SSE front is rather slow and steady, then we would expect to observe a slow and steady seismicity front. On the other hand, if fluid flow is the primary driver, the seismicity typically would expand rapidly first from the initial injection point following the approximate formula of sqrt(t) (Shapiro et al., 1997), where t is time since the initial injection. Examples include the 1975 M_S 7.3 Haicheng foreshock sequence in Northeast China (Lei et al., 2024), the 2008 *M* 4.9 Mogul foreshock sequence in Nevada, USA (Jansen et al., 2019), and the initial foreshocks of the 2021 *M* 6.1 Yangbi

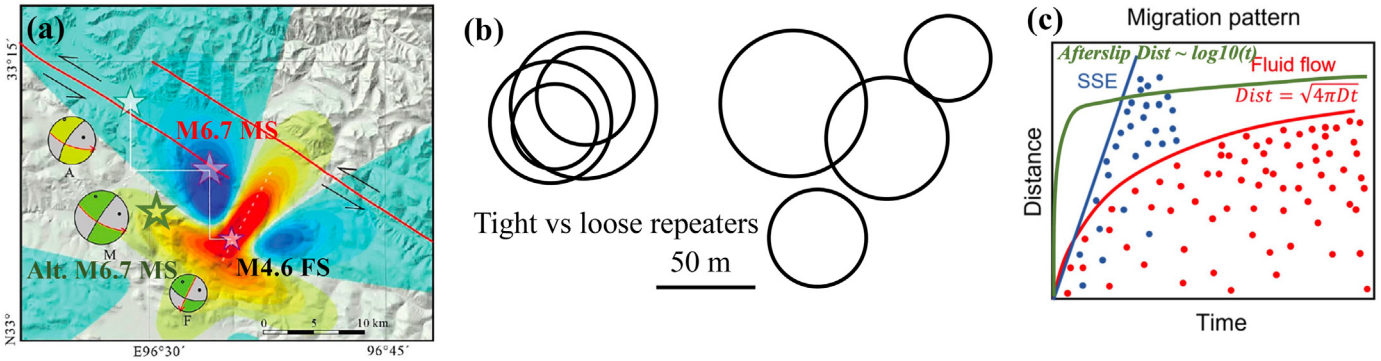

Fig. 5. (a) Static Coulomb stress changes induced by the *M* 4.6 foreshock on the 2010 *M* 6.7 Yushu mainshock epicenter and surrounding region in the Qinghai-Xizang Plateau, Western China (modified from Chuang et al., 2023). The dark green star marks an alternative location of the Yushu mainshock (Huang et al., 2023) where the Coulomb stress change is small but positive. (b) A schematic diagram showing a tight repeating cluster where their source ruptures large overlap, and a loose repeating cluster where their ruptures partially or do not overlap. (c) Expected migration patterns of seismicity driven by a steady-state slow-slip event (SSE), fluid flow, and afterslip. Modified from Zhu et al. (2022a).

sequence (Lei et al., 2021). If a moderate-size foreshock triggers afterslip, which in turn drive its own aftershock activity, then we would expect to observe a very rapid expansion at the beginning following the formula of $\log_{10}(t)$ (Peng and Zhao, 2009; Ross et al., 2017; Perfettini et al., 2018). Examples of such logarithmic-type foreshock-aftershock expansion include the 2011 *M* 9.0 Tohoku-Oki earthquake and its *M* 7.3 foreshock (Kato et al., 2012) and the foreshock sequence of the 2013 *M* 8.1 Iquique earthquake (Kato and Nakagawa, 2014). These different migration/expansion patterns are relatively easy to distinguish if the time scale of observation relatively large. On the other hand, if the time scale is relatively short, such as the half-hour difference between the largest *M* 5.1 foreshock and the *M* 6.1 Yangbi mainshock (Wang et al., 2024a), or if there are multiple fluid injection source points, it is relatively difficult to distinguish between different patterns. We also note that except in a few cases (Schoenball and Ellsworth, 2017; Kato and Obara, 2014; Wu et al., 2017), there is no quantitative way to examine whether a migration pattern would fit either a sqrt(t) or $\log_{10}(t)$ with different expansion speed or diffusivity. Here, the chain of evidence from different aspects becomes crucial.

6. Additional complexities

In addition to the issues mentioned above, in this section we summarize additional complexities that may not be well appreciated in previous studies. First, slow slip is not in steady state, e.g., it could be perturbed by spatial variation of normal stress, or fluid pressure. Based on decades of geodetic and seismological observations, Jolivet and Frank (2020) found that large-scale SSEs consist of many intermittent episodes of short-term bursts. Recent laboratory experiments (Wang et al., 2024c) also showed that the mainshock nucleation process could be intermittently mixed with short accelerating and decelerating episodes. In particular, a later decreasing migration speed of slow slip and foreshocks may result from the shadowing effect of a nearby locked asperity, without requiring afterslip or rate-strengthening rheology. Finally, Im and Avouac (2023) argued that elastic stress interaction in a discrete fault network governed by the rate-and-state-friction can also produce accelerating foreshock sequence and migrating earthquake swarm, without requiring aseismic slip. In other words, the interpretation for observed kinematic features of seismicity migration is not unique. Additionally, migration front of seismicity does not exactly follow the migration front of slow slip or fluid. In many cases, the former could lag the latter (if the latter is considered as the driving force), so only the lower bound of the latter can be estimated from the migration of the former (Yamashita et al., 2022). Possible mechanisms for the time delay include: (1) nucleation of seismicity takes time (Dieterich, 1994), (2) seismicity occurs on asperities, which fail later than the surrounding creep due to their relatively higher normal stress (Ohnaka, 2013). These complexities further highlight the difficulty of identifying the physical mechanism that drive mainshock nucleation based on foreshock seismicity alone, which will be summarized in the next section.

7. Which model(s)?

As summarized before, many progresses have been made in the past decades on observing foreshocks and the mainshock nucleation processes based on field observations (Kato and Ben-Zion, 2021; Martínez-Garzón and Poli, 2024), laboratory experiments (McLaskey, 2019; Bolton et al., 2023; Goebel et al., 2024) and numerical modeling (Cattania and Segall, 2021; He et al., 2023). However, it is still difficult to identify a single physical model that can explain most if not all the observations. The challenges can be summarized as follows.

1. Inconsistent datasets or methods used to identify certain features, which are then used to distinguish between different physical models (Fig. 5). Open sharing of the several recent datasets, such as the 2019 *M* 7.1 Ridgecrest sequence, and the 2024 *M* 7.5 Noto Peninsula sequence, as well as organized efforts such as the community stress drop validation study (Baltay et al., 2024), would allow different groups to compare results and methods with each other to identify potential issues.
2. Additional observations/measurements are needed to distinguish between these models. While seismologists have been trying to use different characteristics of foreshock patterns to distinguish between these models, most observations are indirect and are subject to uncertainties (due to measurement errors, inconsistent methods and inherent insensitivities of seismic waves to these physical processes). For example, while migrating foreshocks (or low-frequency earthquakes/tremor) and repeating earthquakes have been used to infer SSEs (Shelly et al., 2007, 2011; Kato et al., 2012; Uchida and Bürgmann, 2019), the most direct way to observe aseismic slip before large earthquakes is through geodetic measurements (Roeloffs, 2006; Avouac, 2015), which are also subject to high noises and uncertainties (Bletery and Nocquet, 2023, 2024; Bradley and Hubbard, 2023, 2024a). Similarly, while seismic tomographic methods (especially V_P/V_S ratios) can be used to infer the presence of high fluid pressures (Nakajima, 2022), the interpretation is typically not unique. A better way to map fluids in the subsurface is through magnetotelluric (MT) methods (Unsworth and Rondenay, 2013), especially if the spatio-temporal evolution of subsurface fluid flows can be mapped in detail (Shelly, 2024). A combination of different geophysical methods such as temporal changes in seismic velocities (Niu et al., 2008; Wang et al., 2024b), along with geochemical observations (Umeda et al., 2024), hydromechanical modeling (Wang et al., 2024b), may provide us a much more complete picture of how fluid flow, aseismic slip and elastic stress triggering drive foreshocks and mainshock nucleation at seismogenic depth.
3. Some models are end-member types, while others are not mutually exclusive. The *preslip* and *cascade* models (Fig. 2) are clearly end-member models (Martínez-Garzón and Poli, 2024), while the "*cascade-up*" model is a hybrid of these two (McLaskey, 2019). In addition, the three major categories (Fig. 4) of physical processes that drive seismicity (including foreshocks) can co-exist and influence each other. As mentioned before, one of the best examples is the recent 2024 *M* 7.5 Noto Peninsula sequence, where the preceding swarm since 2021 was likely driven by a fluid injection at larger depth, which triggered aseismic processes that lasted for a few years (Nishimura et al., 2023; Kato, 2024). While it is still not clear how the long-lasting swarm changed its mode into a short-term foreshock sequence in the last 4 min before the Noto mainshock, tectonic loading, aseismic slip driven by fluid flow, and elastic stress triggering likely worked in concert (Peng et al., 2025) to trigger the eventual *M* 7.5 mainshock with a very slow initial rupture (Ma et al., 2024; Xu et al., 2024b). From this perspective, the primary mechanisms of different cases can vary over different time scales or spatial ranges (Martínez-Garzón and Poli, 2024). Finally, multiple physical processes can operate simultaneously, as revealed by recent observations of foreshocks (McLaskey, 2019; Yao et al., 2020; Cabrera et al., 2022; Liu et al., 2022; Zhou et al., 2022; Wang et al., 2024a; Martínez-Garzón and Poli, 2024) and aftershocks or triggered seismicity (Meng and Peng, 2014; Ross et al., 2017; Hardebeck et al., 2024). In this perspective, it might not be fruitful to argue which model(s) are correct, because as we all know, "*All models are wrong, but some are useful*" (Box, 1980; Field, 2015). Perhaps we can modify the sentence slightly as "*All models are incomplete, and some work together*".

8. What's next?

While the jury is still out on which physical model(s) play(s) the most important role in driving foreshocks and earthquake nucleation, we have made significant processes over the past few decades on this topic. Looking forward to the upcoming decade, we expect potential

breakthrough in the following directions.

1. **Site-dependent preslip, foreshocks and earthquake predictability.** It is evident that preslip and foreshock activity, which are necessary conditions for large earthquakes, exhibit significant site-specific variability (Mogi, 1963; Roeloffs, 2006; Wetzler et al., 2023). With current observational techniques, the proportion of earthquakes with observable preslip and foreshocks is quite small. However, we expect this number to increase with better instrumentations and better processing methods. On the other hand, it is necessary to systematically identify the practical earthquake predictability of major seismogenic fault systems and develop tailored monitoring, forecasting, and prevention strategies for earthquake hazard in specific space-time windows.
2. **Ultra-dense and near field/deep borehole geophysical observations.** Recent development in ultra-dense sensors such as high-frequency nodal instruments, distributed acoustic sensing (DAS) and other fiber-sensing technologies (Zhan, 2020; Lindsey and Martin, 2021) allow us to observe earthquake sequences in a much higher density than before and simultaneously obtain more detailed source and surrounding structural information through geophysical inversion, which can be used to better image subtle and sub-events before, during and after the mainshock, as well as their relationship with the fine-scale fault structure involved in earthquake nucleation (Shearer et al., 2023; Zhai et al., 2024; Ma et al., 2024). Deep borehole geophysical observations at the North Anatolian Fault in the Eastern Sea of Marmara (GONAF) in Western Türkiye (Kılıç et al., 2020), the BedrettoLab, Swiss Alps (Volpe et al., 2023), the Utah Frontier Observatory for Research in Geothermal Energy (FORGE) (Moore et al., 2019) and elsewhere around the world may provide new insights on the nucleation process of microearthquakes at ultra-fine scale.
3. **Extracting hidden patterns from high-dimensional, high-resolution earthquake catalogs.** In recent years, advanced methods such as template matching (Peng and Zhao, 2009; Zhang and Wen, 2015; Beaucé et al., 2018; Chamberlain et al., 2018) and ML (Kong et al., 2019; Mousavi and Beroza, 2023) have been applied to years of continuous waveforms, resulting in **high-resolution earthquake catalogs** that are several times to tens of times more than listed in standard earthquake catalogs (Ross et al., 2019a; Zhai et al., 2021; Tan et al., 2021; Neves et al., 2023, 2024). These high-resolution catalogs may contain additional information that are not revealed by typical statistical seismology methods such as ETAS. Deep neural point process models (Zhu et al., 2022b; Stockman et al., 2023; Dascher-Cousineau et al., 2023; Zlydenko et al., 2023) have shown promising results that warrant continuing development in this direction. In addition, these high-resolution catalogs (together with focal mechanisms and other derived high-dimensional parameters) can be used to examine how microearthquakes respond to external stress perturbations such as tidal stress and dynamic stress from large distant earthquakes (Li et al., 2023; Wang et al., 2022), which have been shown to evolve before large earthquakes (Beaucé et al., 2023; Lee et al., 2024) and volcanic eruptions (Bell et al., 2021).
4. **Revisiting historical earthquakes.** Major earthquakes are rare and sudden events. On average, around 300 earthquakes of magnitude 6 or greater, 30 of magnitude 7 or greater, and fewer than 2 of magnitude 8 or greater occur worldwide each year. Revisiting historical earthquakes is of special significance. For many past major earthquakes, the understanding of fault structures may have been quite rough due to the limitations of observational technology at that time. For earthquakes with ongoing aftershock activity (e.g., the 1975 Haicheng earthquake), refined data such as precise hypocenters of recent evets recorded by improved networks can enhance our understanding of the mainshock source fault (Chen et al., 2023) and the foreshock mechanisms (Lei et al., 2024). It is also necessary to obtain more detailed physical fields (e.g., high-resolution catalogs) in regions where major earthquakes have occurred in the past with dense array observations and advanced methods as described above, and to compare and analyze the dominant mechanisms of whether and what types of foreshocks occurred (e.g., Manganiello et al., 2023; Wetzler et al., 2023).
5. **Integration of statistical and physical models.** Earthquakes are fundamentally processes where fault rupture release the strain energy accumulated in the surrounding rock volume. The main factors controlling foreshock activity include the fault structure itself, the host rock volume, regional stress field, and potential deep fluids and other transient events that could influence all three of the above factors. These controlling factors evolve independently but with interaction among each other over time. Spatially, they exhibit strong heterogeneity, hierarchical features, and self-similarity, while our understanding of these factors remains uncertain. This results in both physical and statistical models having their respective strengths and limitations. Statistical models, based on empirical relationships of seismic activity, often account for complexity and interactions to some extent. Physical models are generally simplifications of the real-world scenarios and hence may not capture the full complexity. As a result, statistical models are generally more effective than current physical models in reproducing past events and predicting future ones (Mancini et al., 2019; Hardebeck, 2021; Hardebeck et al., 2024). Hence, integrating both approaches is undoubtedly the future direction. In constructing physical models, considerations should extend beyond hydraulics and rock mechanics to include geochemical factors, such as the dissolution and crystallization of fault materials under hydrothermal conditions. Finally, recent numerical modelling results (Xu et al., 2015; Wei et al., 2024) and field observations (Xu et al., 2024a; Wei et al., 2024) suggest a possible phase diagram between self-arresting and runaway earthquake ruptures. This likely indicates a fundamental difference between earthquakes that follow the Gutenberg-Richter frequency-magnitude distribution, and the largest earthquake, i.e., the **dragon-king event** that clearly deviate from the expected Gutenberg-Richter distribution (Ben-Zion, 2008; Sornette and Ouillon, 2012; Sornette et al., 2024). Identifying the physical processes that precede these dragon king events with statistical tools (Beaucé et al., 2023; Lee et al., 2024) and numerical modellings (Wei et al., 2024) can offer new insight into earthquake nucleation, and answer fundamental questions on whether small and large earthquakes start the same or not (Ide, 2019).
6. **Imaging fault zone heterogeneity and fluids.** The heterogeneity of seismogenic faults, including their geometries and frictional properties of fault planes, appears to be one of the necessary conditions for foreshocks and other precursory phenomena (Yamashita et al., 2021; Bolton et al., 2023; Cheng and Wong, 2016; Goebel et al., 2024). Fluid activity, which is episodic in time and localized in space (Lei et al., 2024; Ross et al., 2020), can enhance these heterogeneities, thereby generating observable precursor phenomena (Nishimura et al., 2023). Additionally, this effect causes foreshock activity to be more sensitive to tidal forces, resulting in modulation of their occurrence times (Beaucé et al., 2023; Li et al., 2023; Yu et al., 2022). Therefore, in-depth studies of the heterogeneity of seismogenic structures and fluid effects, along with the related statistical characteristics of seismic activity, may uncover crucial evidence chains for foreshock identification. This should be one of the key directions for future research, can be achieved by high-resolution field studies of exhumed faults (Mitchell and Faulkner, 2009; Ostermeijer et al., 2020) or recent surface ruptures (Barnhart et al., 2020), a combination of high-resolution, high-dimensional earthquake catalogs (Shelly et al., 2023), as well as high-resolution fault zone imaging with advanced recording/methods (Atterholt et al., 2024; Li and Ben-Zion, 2024), possibly in 4D (Wang et al., 2024b).
7. **Integration of research across different scales.** At this point, we have primarily focused on the nucleation and foreshocks of natural earthquakes. Over the past two decades, there has been a continuous increase in seismic activity induced by industrial fluid injection, with

numerous moderate to strong earthquakes observed (e.g. Barbour et al., 2017; Ellsworth et al., 2019; Meng et al., 2021; Liu et al., 2022; Moein et al., 2023; Zhao et al., 2023), comparable in magnitude to typical foreshocks. Compared to natural earthquakes, injection-induced earthquakes offer more detailed known conditions, such as fluid pressure, injection volume, and detailed geological structures. This provides an opportunity for in-depth research on the role of fluids in fault activation. Indeed, this research requires close collaboration between academia, government regulator and industry. The results not only support the safety and efficiency of related industrial operations but also significantly advance the study of precursory processes of fluid-driven or fluid-involved natural earthquakes. The field scale of injection-induced earthquakes lies between laboratory experiments and natural earthquakes, making the integration of research across different scales an important direction.

CRediT authorship contribution statement

Zhigang Peng: Writing – review & editing, Writing – original draft, Visualization, Supervision, Funding acquisition, Conceptualization. **Xinglin Lei:** Writing – review & editing, Visualization, Resources, Formal analysis, Conceptualization.

Declaration of competing interest

Professor Zhigang Peng is the Deputy EIC of EQREA and was not involved in editorial review or the decision to publish this article.

Author agreement and acknowledgement

All authors agree for this publication. This manuscript benefits from useful discussions and comments with Zefeng Li, Shiqing Xu and Changrong He, which greatly improve its quality before submission. We also thank Dr. Kate H. Chen, Qi-Fu Chen, Greg McLaskey, Gerassimos Papadopoulos, Kelin Wang and two anonymous reviewers for their comments during the review/revision process. Z.P. is partially supported by U.S. National Science Foundation grant RISE-2425889.

References

Amezawa, Y., Hiramatsu, Y., Miyakawa, A., Imanishi, K., Otsubo, M., 2023. Long-living earthquake swarm and intermittent seismicity in the northeastern tip of the Noto Peninsula, Japan. Geophys. Res. Lett. 50, e2022GL102670. https://doi.org/10.1029/2022GL102670.

Ampuero, J.-P., Rubin, A.M., 2008. Earthquake nucleation on rate and state faults – aging and slip laws. J. Geophys. Res. 113, B01302. https://doi.org/10.1029/2007JB005082.

Antonioli, A., Belardinelli, M.E., Bizzarri, A., Vogfjord, K.S., 2006. Evidence of instantaneous dynamic triggering during the seismic sequence of year 2000 in south Iceland. J. Geophys. Res. 111, B03302. https://doi.org/10.1029/2005JB003935.

Arrowsmith, S.J., Trugman, D.T., MacCarthy, J., Bergen, K.J., Lumley, D., Magnani, M.B., 2022. Big data seismology. Rev. Geophys. 60 (2), e2021RG000769. https://doi.org/10.1029/2021RG000769.

Atterholt, J., Zhan, Z., Yang, Y., Zhu, W., 2024. Imaging the Garlock Fault Zone with a fiber: A limited damage zone and hidden bimaterial contrast. J. Geophys. Res. Solid Earth 129, e2024JB028900. https://doi.org/10.1029/2024JB028900.

Avouac, J.P., 2015. From geodetic imaging of seismic and aseismic fault slip to dynamic modeling of the seismic cycle. Annu. Rev. Earth Planet Sci. 43 (1), 233–271. https://doi.org/10.1146/annurev-earth-060614-105302.

Bakun, W.H., McEvilly, T.V., 1979. Earthquakes near Parkfield, California: comparing the 1934 and 1966 sequences. Science 205 (4413), 1375–1377. https://doi.org/10.1126/science.205.4413.1375.

Bakun, W.H., Lindh, A.G., 1985. The Parkfield, California, earthquake prediction experiment. Science 229, 619–624. https://doi.org/10.1126/science.229.4714.619.

Bakun, W.H., Aagaard, B., Dost, B., Ellsworth, W.L., Hardebeck, J.L., Harris, R.A., Ji, C., Johnston, M.J., Langbein, J., Lienkaemper, J.J., Michael, A.J., 2005. Implications for prediction and hazard assessment from the 2004 Parkfield earthquake. Nature 437 (7061), 969–974. https://doi.org/10.1038/nature04067.

Baltay, A., Abercrombie, R., Chu, S., Taira, T., 2024. The SCEC/USGS community stress drop validation study using the 2019 Ridgecrest earthquake sequence. Seismica 3 (1). https://doi.org/10.26443/seismica.v3i1.1009.

Barbour, A.J., Norbeck, J.H., Rubinstein, J.L., 2017. The effects of varying injection rates in Osage County, Oklahoma, on the 2016 Mw 5.8 Pawnee earthquake. Seismol Res. Lett. 88, 1040–1053. https://doi.org/10.1785/0220170003.

Barcheck, G., Brodsky, E.E., Fulton, P.M., King, M.A., Siegfried, M.R., Tulaczyk, S., 2021. Migratory earthquake precursors are dominant on an ice stream fault. Science Advance 7 (6), eabd0105. https://doi.org/10.1126/sciadv.abd0105.

Barnhart, W.D., Gold, R.D., Hollingsworth, J., 2020. Localized fault-zone dilatancy and surface inelasticity of the 2019 Ridgecrest earthquakes. Nat. Geosci. 13, 699–704. https://doi.org/10.1038/s41561-020-0628-8.

Beaucé, E., Frank, W.B., Romanenko, A., 2018. Fast matched filter (FMF): an efficient seismic matched-filter search for both CPU and GPU architectures. Seismol Res. Lett. 89 (1), 165–172. https://doi.org/10.1785/0220170181.

Beaucé, E., Poli, P., Waldhauser, F., Holtzman, B., Scholz, C., 2023. Enhanced tidal sensitivity of seismicity before the 2019 magnitude 7.1 Ridgecrest, California earthquake. Geophys. Res. Lett. 50, e2023GL104375. https://doi.org/10.1029/2023GL104375.

Bedford, J., Moreno, M., Schurr, B., Bartsch, M., Oncken, O., 2015. Investigating the final seismic swarm before the Iquique-Pisagua 2014 Mw 8.1 by comparison of continuous GPS and seismic foreshock data. Geophys. Res. Lett. 42, 3820–3828. https://doi.org/10.1002/2015GL063953.

Beeler, N.M., Lockner, D.L., Hickman, S.H., 2001. A simple stick-slip and creep-slip model for repeating earthquakes and its implication for microearthquakes at Parkfield. Bull. Seismol. Soc. Am. 91, 1797–1804. https://doi.org/10.1785/0120000096.

Bell, A.F., Hernandez, S., McCloskey, J., Ruiz, M., LaFemina, P.C., Bean, C.J., Möllhoff, M., 2021. Dynamic earthquake triggering response tracks evolving unrest at Sierra Negra volcano, Galápagos Islands. Sci. Adv. 7 (39), eabh0894. https://doi.org/10.1126/sciadv.abh0894.

Ben-Zion, Y., 2008. Collective behavior of earthquakes and faults: continuum-discrete transitions, progressive evolutionary changes, and different dynamic regimes. Rev. Geophys. 46, RG4006. https://doi.org/10.1029/2008RG000260.

Ben-Zion, Y., Beroza, G.C., Bohnhoff, M., Gabriel, A.A., Mai, P.M., 2022. A grand challenge international infrastructure for earthquake science. Seismol Res. Lett. 93 (6), 2967–2968. https://doi.org/10.1785/0220220266.

Beroza, G.C., Segou, M., Mousavi, S.M., 2021. Machine learning and earthquake forecasting—next steps. Nat. Commun. 12 (1), 4761. https://doi.org/10.1038/s41467-021-24952-6.

Bletery, Q., Nocquet, J.-M., 2023. The precursory phase of large earthquakes. Science 381 (6655), 297–301. https://doi.org/10.1126/science.adg2565, 2023.

Bletery, Q., Nocquet, J.-M., 2025. Do large earthquakes start with a precursory phase of slow slip? Seismica 3 (2). https://doi.org/10.31223/X5RT3N.

Bolton, D.C., Marone, C., Saffer, D., Trugman, D.T., 2023. Foreshock properties illuminate nucleation processes of slow and fast laboratory earthquakes. Nat. Commun. 14, 3859. https://doi.org/10.1038/s41467-023-39399-0.

Bouchon, M., Karabulut, H., Aktar, M., Özalaybey, S., Schmittbuhl, J., Bouin, M.-P., 2011. Extended nucleation of the 1999 Mw 7.6 Izmit earthquake. Science 331 (6019), 877–880. https://doi.org/10.1126/science.1197341.

Bouchon, M., Durand, V., Marsan, D., Karabulut, H., Schmittbuhl, J., 2013. The long precursory phase of most large interplate earthquakes. Nat. Geosci. 6 (4), 299–302. https://doi.org/10.1038/ngeo1770.

Box, G.E.P., 1980. Sampling and Bayes inference in scientific modelling and robustness. J. Roy Stat. Soc. Ser. A 143, 383–430. https://doi.org/10.2307/2982063.

Bradley, K., Hubbard, J., 2023. Earthquake precursors? not so fast. Earthquake Insights. https://doi.org/10.62481/310cc439.

Bradley, K., Hubbard, J., 2024a. Precursory slip before large earthquakes - signal or noise? Earthquake Insights. https://doi.org/10.62481/0ff960fa.

Bradley, K., Hubbard, J., 2024b. Does this machine learning model predict large earthquakes? Maybe not. Earthquake Insights. https://doi.org/10.62481/e64960d4.

Bürgmann, R., 2018. The geophysics, geology and mechanics of slow fault slip. Earth Planet Sci. Lett. 495, 112–134. https://doi.org/10.1016/j.epsl.2018.04.062.

Cabrera, L., Poli, P., Frank, W.B., 2022. Tracking the spatio-temporal evolution of foreshocks preceding the Mw 6.1 2009 L'Aquila earthquake. J. Geophys. Res. Solid Earth 127, e2021JB023888. https://doi.org/10.1029/2021JB023888.

Cattania, C., Segall, P., 2021. Precursory slow slip and foreshocks on rough faults. J. Geophys. Res. Solid Earth 126 (4), e2020JB020430. https://doi.org/10.1029/2020JB020430.

Chamberlain, C.J., Hopp, C.J., Boese, C.M., Warren-Smith, E., Chambers, D., Chu, S.X., Michailos, K., Townend, J., 2018. EQcorrscan: repeating and near-repeating earthquake detection and analysis in Python. Seismol Res. Lett. 89 (1), 173–181. https://doi.org/10.1785/0220170151.

Chen, H., Han, P., Hattori, K., 2022. Recent advances and challenges in the seismo-electromagnetic study: a brief review. Rem. Sens. 14 (22), 5893. https://doi.org/10.3390/rs14225893.

Chen, K.H., Bürgmann, R., Nadeau, R.M., Chen, T., Lapusta, N., 2010. Postseismic variations in seismic moment and recurrence interval of repeating earthquakes. Earth Planet Sci. Lett. 299 (1–2), 118–125. https://doi.org/10.1016/j.epsl.2010.08.027.

Chen, L., Luo, P., Fu, H., Cai, J., Liu, X., Yang, J., Li, Y., Lei, S., Shen, B., Liu, Z., 1997. Medium-term, short-term and impending predictions and features precursory anomalies for the M = 7.3 earthquake happened at Menglian of Yunnan near the China-Burma border. J. Earthq. Pred. Res. 6 (1), 73–87.

Chen, Q.F., Wang, K., 2010. The 2008 Wenchuan earthquake and earthquake prediction in China. Bull. Seismol. Soc. Am. 100 (5B), 2840–2857. https://doi.org/10.1785/0120090314.

Chen, Q.F., Li, L., 2018. Deep deformation of the Longmenshan fault zone related to the 2008 Wenchuan earthquake. Chin. Sci. Bull. 63 (19), 1917–1933. https://doi.org/10.1360/n972018-00362.

Chen, W., Neves, M., Zhai, Q., Daniels, C., Adeboboye, O., Jaume, S., Peng, Z., 2023. Preliminary results from a dense short-period seismic deployment around the source zone of the 1886 M 7 South Carolina earthquake. Seismol Res. Lett. 94 (5), 2479–2488. https://doi.org/10.1785/0220230085.

Chen, X., Shearer, P.M., 2016. Analysis of foreshock sequences in California and implications for earthquake triggering. Pure Appl. Geophys. 173, 133–152. https://doi.org/10.1007/s00024-015-1103-0.
Chen, Y., Liu, J., Ge, H., 1999. Pattern characteristics of foreshock sequences. In: Wyss, M., Shimazaki, K., Ito, A. (Eds.), Seismicity Patterns, Their Statistical Significance and Physical Meaning. PAGEOPH Topical Volumes. Birkhäuser, Basel. https://doi.org/10.1007/978-3-0348-8677-2_10.
Cheng, Y., Wong, L.N.Y., 2016. Occurrence of foreshocks in large earthquakes with strike-slip rupturing. Bull. Seismol. Soc. Am. 106, 213–224. https://doi.org/10.1785/0120140338.
Christophersen, A., Smith, E.G., 2008. Foreshock rates from aftershock abundance. Bull. Seismol. Soc. Am. 98 (5), 2133–2148. https://doi.org/10.1785/0120060143.
Chuang, L.Y., Peng, Z., Lei, X., Wang, B., Liu, J., Zhai, Q., Tu, H., 2023. Foreshocks of the 2010 Mw 6.7 Yushu, China Earthquake occurred near an extensional step-over. J. Geophys. Res. Solid Earth 128, e2022JB025176. https://doi.org/10.1029/2022JB025176.
Chung, W.Y., Cipar, J.J., 1983. Source modeling of the Hsingtai, China earthquakes of March 1966. Phys. Earth Planet. In. 33 (2), 111–125. https://doi.org/10.1016/0031-9201(83)90144-9.
Cocco, M., Aretusini, S., Cornelio, C., Nielsen, S.B., Spagnuolo, E., Tinti, E., Di Toro, G., 2023. Fracture energy and breakdown work during earthquakes. Annu. Rev. Earth Planet Sci. 51 (1), 217–252. https://doi.org/10.1146/annurev-earth-071822-100304.
Dascher-Cousineau, K., Lay, T., Brodsky, E.E., 2020. Two foreshock sequences post Gulia and wiemer (2019). Seismol Res. Lett. 91 (5), 2843–2850. https://doi.org/10.1785/0220200082.
Dascher-Cousineau, K., Shchur, O., Brodsky, E.E., Günnemann, S., 2023. Using deep learning for flexible and scalable earthquake forecasting. Geophys. Res. Lett. 50, e2023GL103909. https://doi.org/10.1029/2023GL103909.
Deng, Y., Peng, Z., Liu-Zeng, J., 2020. Systematic search for repeating earthquakes along the haiyuan fault system in northeastern Tibet. J. Geophys. Res. 125, e2020JB019583. https://doi.org/10.1029/2020JB019583.
Dieterich, J.H., 1992. Earthquake nucleation on faults with rate-and state-dependent strength. Tectonophysics 211 (1–4), 115–134. https://doi.org/10.1016/0040-1951(92)90055-B.
Dieterich, J., 1994. A constitutive law for rate of earthquake production and its application to earthquake clustering. J. Geophys. Res. 99 (B2), 2601–2618. https://doi.org/10.1029/93JB02581.
Ding, X., Xu, S., Xie, Y., van den Ende, M., Premus, J., Ampuero, J.-P., 2023. The sharp turn: backward rupture branching during the 2023 Mw 7.8 Kahramanmaraş (Türkiye) earthquake. Seismica 2 (3). https://doi.org/10.26443/seismica.v2i3.1083.
Dodge, D.A., Beroza, G.C., Ellsworth, W.L., 1996. Detailed observations of California foreshock sequences: implications for the earthquake initiation process. J. Geophys. Res. Solid Earth 101 (B10), 22371–22392. https://doi.org/10.1029/96JB02269.
Dong, P., Chen, R., Xia, K., Yao, W., Peng, Z., Elsworth, D., 2024. Earthquake delay and rupture velocity in near-field dynamic triggering dictated by stress-controlled nucleation. Seismological Society of America 94 (2A), 913–924. https://doi.org/10.1785/0220220264.
Ellsworth, W.L., 2019. From foreshocks to mainshocks: mechanisms and implications for earthquake nucleation and rupture propagation. In: Mechanics of Earthquake Faulting. IOS Press, pp. 95–112. https://doi.org/10.3254/978-1-61499-979-9-95.
Ellsworth, W.L., Giardini, D., Townend, J., Ge, S., Shimamoto, T., 2019. Triggering of the pohang, korea, earthquake (Mw 5.5) by enhanced geothermal system stimulation. Seismol Res. Lett. 90 (5), 1844–1858. https://doi.org/10.1785/0220190102.
Ellsworth, W.L., Bulut, F., 2018. Nucleation of the 1999 Izmit earthquake by a triggered cascade of foreshocks. Nat. Geosci. 11 (7), 531–535. https://doi.org/10.1038/s41561-018-0145-1.
Felzer, K.R., Abercrombie, R.E., Ekström, G., 2004. A common origin for aftershocks, foreshocks, and multiplets. Bull. Seismol. Soc. Am. 94 (1), 88–98. https://doi.org/10.1785/0120030069.
Felzer, K.R., Page, M., Michael, A., 2015. Artificial seismic acceleration. Nature Geosci 8, 82–83. https://doi.org/10.1038/ngeo2358.
Field, E.H., 2015. All models are wrong, but some are useful. Seismol Res. Lett. 86 (2A), 291–293. https://doi.org/10.1785/02201401213.
Freed, A.M., 2005. Earthquake triggering by static, dynamic, and postseismic stress transfer. Annu. Rev. Earth Planet Sci. 33 (1), 335–367. https://doi.org/10.1146/annurev.earth.33.092203.122505.
Freund, F., 2011. Pre-earthquake signals: underlying physical processes. J. Asian Earth Sci. 41 (4–5), 383–400. https://doi.org/10.1016/j.jseaes.2010.03.009.
Fukushima, Y., Nishikawa, T., Kano, Y., 2023. High probability of successive occurrence of Nankai megathrust earthquakes. Sci. Rep. 13, 63. https://doi.org/10.1038/s41598-022-26455-w.
Gabriel, A.A., Garagash, D.I., Palgunadi, K.H., Mai, P.M., 2024. Fault size–dependent fracture energy explains multiscale seismicity and cascading earthquakes. Science 385 (6707), eadj9587. https://doi.org/10.1126/science.adj9587.
Gao, D., Kao, H., Wang, B., 2021. Misconception of waveform similarity in the identification of repeating earthquakes. Geophys. Res. Lett. 48, e2021GL092815. https://doi.org/10.1029/2021GL092815.
Ge, S., Saar, M.O., 2022. Induced seismicity during geoenergy development—a hydromechanical perspective. J. Geophys. Res. Solid Earth 127, e2021JB023141. https://doi.org/10.1029/2021JB023141.
Girona, T., Drymoni, K., 2024. Abnormal low-magnitude seismicity preceding large-magnitude earthquakes. Nat. Commun. 15, 7429. https://doi.org/10.1038/s41467-024-51596-z.
Goebel, T.H., Schuster, V., Kwiatek, G., Pandey, K., Dresen, G., 2024. A laboratory perspective on accelerating preparatory processes before earthquakes and implications for foreshock detectability. Nat. Commun. 15 (1), 5588. https://doi.org/10.1038/s41467-024-49959-7.
Goltz, J.D., 2015. A further note on operational earthquake forecasting: an emergency management perspective. Seismol Res. Lett. 86 (5), 1231–1233. https://doi.org/10.1785/0220150080.
Guérin-Marthe, S., Nielsen, S., Bird, R., Giani, S., Di Toro, G., 2019. Earthquake nucleation size: Evidence of loading rate dependence in laboratory faults. J. Geophys. Res. Solid Earth 124 (1), 689–708. https://doi.org/10.1029/2018JB016803.
Gulia, L., Wiemer, S., 2019. Real-time discrimination of earthquake foreshocks and aftershocks. Nature 574, 193–199. https://doi.org/10.1038/s41586-019-1606-4.
Gutenberg, B., Richter, C.F., 1944. Frequency of earthquakes in California. Bull. Seismol. Soc. Am. 4, 185–188. https://doi.org/10.1785/BSSA0340040185.
Hauksson, E., Stock, J., Hutton, K., Yang, W., Vidal-Villegas, J.A., Kanamori, H., 2011. The 2010 M w 7.2 El Mayor-Cucapah earthquake sequence, Baja California, Mexico and southernmost California, USA: active seismotectonics along the Mexican pacific margin. Pure Appl. Geophys. 168, 1255–1277. https://doi.org/10.1007/s00024-010-0209-7.
Hardebeck, J.L., 2021. Spatial clustering of aftershocks impacts the performance of physics-based earthquake forecasting models. J. Geophys. Res. Solid Earth 126, e2020JB020824. https://doi.org/10.1029/2020JB020824.
Hardebeck, J.L., Llenos, A.L., Michael, A.J., Page, M.T., Schneider, M., van der Elst, N.J., 2024. Aftershock forecasting. Annu. Rev. Earth Planet Sci. 52. https://doi.org/10.1146/annurev-earth-040522-102129.
Harris, R.A., 2017. Large earthquakes and creeping faults. Rev. Geophys. 55 (1), 169–198. https://doi.org/10.1002/2016RG000539.
He, C., Zhang, L., Liu, P., Chen, Q.-F., 2023. Characterizing the final stage of simulated earthquake nucleation governed by rate-and-state fault friction. J. Geophys. Res. Solid Earth 128, e2023JB026422. https://doi.org/10.1029/2023JB026422.
Helmstetter, A., Sornette, D., Grasso, J.R., 2003. Mainshocks are aftershocks of conditional foreshocks: how do foreshock statistical properties emerge from aftershock laws. J. Geophys. Res. Solid Earth 108 (B1), 2046. https://doi.org/10.1029/2002JB001991.
Hill, D.P., Prejean, S., 2015. Dynamic triggering. In: Kanamori, H. (Ed.), Treatise on Geophysics, second ed., vol. 4. Elsevier, Amsterdam, The Netherlands. https://doi.org/10.1016/B978-0-444-53802-4.00078-6.
Hirose, F., Miyaoka, K., Hayashimoto, N., Yamazaki, T., Nakamura, M., 2011. Outline of the 2011 off the Pacific coast of Tohoku Earthquake (Mw 9.0) - seismicity: foreshocks, mainshock, aftershocks, and induced activity-. Earth Planets Space 63, 513–518. https://doi.org/10.5047/eps.2011.05.019.
Hirose, H., Kato, A., Kimura, T., 2024. Did short-term preseismic crustal deformation precede the 2011 great Tohoku-Oki earthquake? An examination of stacked tilt records. Geophys. Res. Lett. 51 (12), e2024GL109384. https://doi.org/10.1029/2024GL109384.
Huang, F., Li, M., Ma, Y., Han, Y., Tian, L., Yan, W., Li, X., 2017. Studies on earthquake precursors in China: a review for recent 50 years. Geodesy and Geodynamics 8 (1), 1–12. https://doi.org/10.1016/j.geog.2016.12.002.
Huang, H., Meng, L., Bürgmann, R., Wang, W., Wang, K., 2020. Spatio-temporal foreshock evolution of the 2019 M 6.4 and M 7.1 Ridgecrest, California earthquakes. Earth Planet Sci. Lett. 551, 116582. https://doi.org/10.1016/j.epsl.2020.116582.
Huang, Y., Li, H., Ma, Y., Ma, J., 2023. Long-term spatial–temporal evolution of seismicity of the 2010 Ms 7.1 Yushu, Qinghai, China earth- quake. IEEE Trans. Geosci. Rem. Sens. 61, 1–9. https://doi.org/10.1109/TGRS.2022.3231878.
Hudnut, K.W., Seeber, L., Pacheco, J., 1989. Cross-fault triggering in the November 1987 Superstition Hills earthquake sequence, southern California. Geophys. Res. Lett. 16 (2), 199–202. https://doi.org/10.1029/GL016i002p00199.
Ide, S., 2019. Frequent observations of identical onsets of large and small earthquakes. Nature 573, 112–116. https://doi.org/10.1038/s41586-019-1508-5.
Ide, S., Beroza, G.C., 2023. Slow earthquake scaling reconsidered as a boundary between distinct modes of rupture propagation. Proc. Natl. Acad. Sci. USA 120 (32), e2222102120. https://doi.org/10.1073/pnas.2222102120.
Im, K., Avouac, J.-P., 2023. Cascading foreshocks, aftershocks and earthquake swarms in a discrete fault network. Geophys. J. Int. 235 (1), 831–852. https://doi.org/10.1093/gji/ggad278.
Ishikawa, Y., Bai, L., 2024. The 2024 Mj7.6 Noto Peninsula, Japan earthquake caused by the fluid flow in the crust. Earthquake Research Advances 2024, 100292. https://doi.org/10.1016/j.eqrea.2024.100292, 547.
Ito, R., Kaneko, Y., 2023. Physical mechanism for a temporal decrease of the Gutenberg-Richter b-value prior to a large earthquake. J. Geophys. Res. Solid Earth 128, e2023JB027413. https://doi.org/10.1029/2023JB027413.
Ito, Y., Hino, R., Kido, M., Fujimoto, H., Osada, Y., Inazu, D., Ohta, Y., Iinuma, T., Ohzono, M., Miura, S., Mishina, M., 2013. Episodic slow slip events in the Japan subduction zone before the 2011 Tohoku-Oki earthquake. Tectonophysics 600, 14–26. https://doi.org/10.1016/j.tecto.2012.08.022.
Itoh, Y., Socquet, A., Radiguet, M., 2023. Largest aftershock nucleation driven by afterslip during the 2014 Iquique sequence. Geophys. Res. Lett. 50, e2023GL104852. https://doi.org/10.1029/2023GL104852.
Jansen, G., Ruhl, C.J., Miller, S.A., 2019. Fluid pressure-triggered foreshock sequence of the 2008 Mogul earthquake sequence: insights from stress inversion and numerical modeling. J. Geophys. Res. Solid Earth 124, 3744–3765. https://doi.org/10.1029/2018JB015897.
Jia, K., Zhou, S., Zhuang, J., Jiang, C., Guo, Y., Gao, Z., Gao, S., Ogata, Y., Song, X., 2020. Nonstationary background seismicity rate and evolution of stress changes in the changning salt mining and shale-gas hydraulic fracturing region, Sichuan Basin, China. Seismol Res. Lett. 91 (4), 2170–2181. https://doi.org/10.1785/0220200092.
Jolivet, R., Frank, W.B., 2020. The transient and intermittent nature of slow slip. AGU Advances 1, e2019AV000126. https://doi.org/10.1029/2019AV000126.

Jones, L.M., Wang, B., Xu, S., Fitch, T.J., 1982. The foreshock sequence of the february 4, 1975, Haicheng earthquake (M = 7.3). J. Geophys. Res. 87 (B6), 4575–4584. https://doi.org/10.1029/JB087iB06p04575.
Jordan, T.H., Jones, L.M., 2010. Operational earthquake forecasting: some thoughts on why and how. Seismol Res. Lett. 81, 571–574. https://doi.org/10.1785/gssrl.81.4.571.
Jordan, T.H., Chen, Y.-T., Gasparini, P., Madariaga, R., Main, I., Marzocchi, W., Papadopoulos, G., Sobolev, G., Yamaoka, K., Zschau, J., 2011. Operational earthquake forecasting: state of knowledge and guidelines for implementation, final report of the international commission on earthquake forecasting for civil protection. Ann. Geophys. 54 (4), 315–391. https://doi.org/10.4401/ag-5350.
Jordan, T.H., Marzocchi, W., Michael, A.J., Gerstenberger, M.C., 2014. Operational earthquake forecasting can enhance earthquake preparedness. Seismol Res. Lett. 85 (5), 955–959. https://doi.org/10.1785/0220140143.
Kanamori, H., 1981. The nature of seismicity patterns before large earthquakes. In: Simpson, D.W., Richards, P.G. (Eds.), Earthquake Prediction. https://doi.org/10.1029/ME004p0001.
Kanamori, H., 2003. Earthquake prediction: an overview. Int. Geophys. 81, 1205–1216. https://doi.org/10.1016/S0074-6142(03)80186-9.
Kanamori, H., Brodsky, E.E., 2004. The physics of earthquakes. Rep. Prog. Phys. 67 (8), 1429. https://doi.org/10.1088/0034-4885/67/8/R03.
Kaneko, Y., Lapusta, N., 2008. Variability of earthquake nucle-ation in continuum models of rate-and-state faults and implications for aftershock rates. J. Geophys. Res. 113, B12312. https://doi.org/10.1029/2007JB005154.
Kato, A., 2019. The evolution of fault slip rate prior to earthquake: the role of slow-and fast-slip modes. In: Mechanics of Earthquake Faulting, vols. 53–80. IOS Press. https://doi.org/10.3254/978-1-61499-979-9-53.
Kato, A., 2024. Implications of fault-valve behavior from immediate aftershocks following the 2023 Mj6.5 earthquake beneath the Noto Peninsula, central Japan. Geophys. Res. Lett. 51, e2023GL106444. https://doi.org/10.1029/2023GL106444.
Kato, A., Obara, K., Igarashi, T., Tsuruoka, H., Nakagawa, S., Hirata, N., 2012. Propagation of slow slip leading up to the 2011 Mw 9.0 Tohoku-Oki earthquake. Science 335 (6069), 705–708. https://doi.org/10.1126/science.1215141.
Kato, A., Obara, K., 2014. Step-like migration of early aftershocks following the 2007 Mw 6.7 Noto-Hanto earthquake, Japan. Geophys. Res. Lett. 41, 3864–3869. https://doi.org/10.1002/2014GL060427.
Kato, A., Nakagawa, S., 2014. Multiple slow-slip events during a foreshock sequence of the 2014 Iquique, Chile Mw 8.1 earthquake. Geophys. Res. Lett. 41 (15), 5420–5427. https://doi.org/10.1002/2014GL061138.
Kato, A., Fukuda, J., Nakagawa, S., Obara, K., 2016. Foreshock migration preceding the 2016 Mw 7.0 Kumamoto earthquake, Japan. Geophys. Res. Lett. 43, 8945–8953. https://doi.org/10.1002/2016GL070079.
Kato, A., Ben-Zion, Y., 2021. The generation of large earthquakes. Nat. Rev. Earth Environ. 2, 26–39. https://doi.org/10.1038/s43017-020-00108-w.
Kılıç, T., Kartal, R.F., Kadirioğlu, F.T., Bohnhoff, M., Nurlu, M., Acarel, D., Garzon, P.M., Dresen, G., Özsarac, V., Malin, P.E., 2020. Geophysical borehole observatory at the North Anatolian Fault in the Eastern Sea of Marmara (GONAF): initial results. J. Seismol. 24, 375–395. https://doi.org/10.1007/s10950-020-09907-6.
Kong, Q., Trugman, D.T., Ross, Z.E., Bianco, M.J., Meade, B.J., Gerstoft, P., 2019. Machine learning in seismology: Turning data into insights. Seismol Res. Lett. 90 (1), 3–14. https://doi.org/10.1785/0220180259.
Kwiatek, G., Martínez-Garzón, P., Becker, D., Dresen, G., Cotton, F., Beroza, G.C., Acarel, D., Ergintav, S., Bohnhoff, M., 2023. Months-long seismicity transients preceding the 2023 M_W 7.8 Kahramanmaraş earthquake, Türkiye. Nat. Commun. 14 (1), 7534. https://doi.org/10.1038/s41467-023-42419-8.
Langbein, J., Borcherdt, R., Dreger, D., Fletcher, J., Hardebeck, J.L., Hellweg, M., Ji, C., Johnston, M., Murray, J.R., Nadeau, R., Rymer, M.J., 2005. Preliminary report on the 28 september 2004, M 6.0 Parkfield, California earthquake. Seismol Res. Lett. 76 (1), 10–26. https://doi.org/10.1785/gssrl.76.1.10.
Lee, J., Tsai, V.C., Hirth, G., Chatterjee, A., Trugman, D.T., 2024. Fault-network geometry influences earthquake frictional behaviour. Nature 631, 106–110. https://doi.org/10.1038/s41586-024-07518-6.
Lei, X., 2003. How do asperities fracture? An experimental study of unbroken asperities. Earth Planet Sci. Lett. 213, 347–359. https://doi.org/10.1016/S0012-821X(03)00328-5.
Lei, X., 2024. Fluid-driven Fault Nucleation, Rupture Processes, and Permeability Evolution in Oshima Granite—Preliminary Results and Acoustic Emission Datasets. Geohazard Mechanics. https://doi.org/10.1016/j.ghm.2024.04.003.
Lei, X., Ma, S., 2014. Laboratory acoustic emission study for earthquake generation process. Earthq. Sci. 27, 627–646. https://doi.org/10.1007/s11589-014-0103-y.
Lei, X., Wang, Z., Su, J., 2019. The december 2018 ML 5.7 and january 2019 ML 5.3 earthquakes in south Sichuan Basin induced by shale gas hydraulic fracturing. Seismol Res. Lett. 90, 1099–1110. https://doi.org/10.1785/0220190029.
Lei, X., Su, J., Wang, Z., 2020. Growing seismicity in the Sichuan Basin and its association with industrial activities. Sci. China Earth Sci. 63, 1633–1660. https://doi.org/10.1007/s11430-020-9646-x.
Lei, X., Wang, Z., Ma, S., He, C., 2021. A preliminary study on the characteristics and mechanism of the May 2021 MS 6.4 Yangbi earthquake sequence, Yunnan, China. Acta Seismologica Sinica 43 (3), 261. https://doi.org/10.11939/jass.20210100.
Lei, X., Wang, Z., Ma, S., He, C., 2024. Step-over of strike-slip faults and overpressure fluid favor occurrence of foreshocks: insights from the 1975 Haicheng fore-main-aftershock sequence, China. Earthq. Res. Adv. 100237. https://doi.org/10.1016/j.eqrea.2023.100237.
Li, C., Peng, Z., Yao, D., Meng, X., Zhai, Q., 2023. Temporal changes of seismicity in Salton Sea Geothermal Field due to distant earthquakes and geothermal productions. Geophys. J. Int. 232 (1), 287–299. https://doi.org/10.1093/gji/ggac324.
Li, G., Ben-Zion, Y., 2024. Multi-scale seismic imaging of the Ridgecrest, CA, region with waveform inversion of regional and dense array data. J. Geophys. Res. Solid Earth 129, e2023JB028149. https://doi.org/10.1029/2023JB028149.
Li, H., 1996. China's campaign to predict quakes. Science 273, 1484–1486. https://doi.org/10.1126/science.273.5281.1484.
Li, L., Chen, Q.f., Niu, F., Su, J., 2011. Deep slip rates along the Longmen Shan fault zone estimated from repeating microearthquakes. J. Geophys. Res. Solid Earth 116, B09310. https://doi.org/10.1029/2011JB008406.
Li, L., Wang, B., Peng, Z., Hou, J., Wang, F., 2024a. Statistical features of seismicity associated with large earthquakes on the Chinese continent between 2008 and 2019 based on newly detected catalogs. Seismol Res. Lett. 95, 1701–1717. https://doi.org/10.1785/0220230189.
Li, M., Niemeijer, A., van Dinther, Y., 2024b. Earthquake nucleation and slip behavior altered by stochastic normal stress heterogeneity. ESS Open Archive. https://doi.org/10.22541/essoar.172108738.88404748/v1.
Lin, C.H., 2009. Foreshock characteristics in Taiwan: potential earthquake warning. J. Asian Earth Sci. 34 (5), 655–662. https://doi.org/10.1016/j.jseaes.2008.09.006.
Lin, R., 2003. Predictions and social response capacities in face of the 1995 Menglian earthquake (M = 7.3): an overview. Early Warning Systems for Natural Disaster Reduction. Springer, Berlin, Heidelberg, pp. 481–486. https://doi.org/10.1007/978-3-642-55903-7_63.
Lindsey, N.J., Martin, E.R., 2021. Fiber-optic seismology. Annu. Rev. Earth Planet Sci. 49 (1), 309–336. https://doi.org/10.1146/annurev-earth-072420-065213.
Liu, M., Li, H., Li, L., Zhang, M., Wang, W., 2022. Multistage nucleation of the 2021 Yangbi MS 6.4 earthquake, Yunnan, China and its foreshocks. J. Geophys. Res. Solid Earth 127, e2022JB024091. https://doi.org/10.1029/2022JB024091.
Liu, Y., McGuire, J.J., Behn, M.D., 2020. Aseismic Transient Slip on the Gofar Transform Fault, East Pacific Rise. Proceedings of the National Academy of Sciences 117 (19), 10188–10194. https://doi.org/10.1073/pnas.1913625117.
Lu, C., Zhou, X., Chen, Z., Liu, Z., Hu, L., Sun, F., Martinelli, G., Li, Y., 2023. Earthquake geochemical scientific expedition and research. Earthquake Research Advances 3 (4), 100239. https://doi.org/10.1016/j.eqrea.2023.100239.
Ma, K.F., von Specht, S., Kuo, L.W., Huang, H.H., Lin, C.R., Lin, C.J., Ku, C.S., Wu, E.S., Wang, C.Y., Chang, W.Y., Jousset, P., 2024. Broad-band strain amplification in an asymmetric fault zone observed from borehole optical fiber and core. Communications Earth & Environment 5 (1), 402. https://doi.org/10.1038/s43247-024-01558-6.
Maeda, K., 1999. Time distribution of immediate foreshocks obtained by a stacking method. Pure Appl. Geophys. 155, 381–394. https://doi.org/10.1007/s000240050270.
Mancini, S., Segou, M., Werner, M.J., Cattania, C., 2019. Improving physics-based aftershock forecasts during the 2016–2017 Central Italy earthquake cascade. J. Geophys. Res. Solid Earth 124, 8626–8643. https://doi.org/10.1029/2019JB017874.
Manganiello, E., Herrmann, M., Marzocchi, W., 2023. New physical implications from revisiting foreshock activity in southern California. Geophys. Res. Lett. 50, e2022GL098737. https://doi.org/10.1029/2022GL098737.
Martínez-Garzón, P., Poli, P., 2024. Cascade and preslip models oversimplify the complexity of earthquake preparation in nature. Commun. Earth Environ. 5, 120. https://doi.org/10.1038/s43247-024-01285-y.
Marty, S., Schubnel, A., Bhat, H.S., Aubry, J., Fukuyama, E., Latour, S., Nielsen, S., Madariaga, R., 2023. Nucleation of laboratory earthquakes: quantitative analysis and scalings. J. Geophys. Res. Solid Earth 128, e2022JB026294. https://doi.org/10.1029/2022JB026294.
Materna, K., Taira, T., Bürgmann, R., 2018. Aseismic transform fault slip at the Mendocino Triple Junction from characteristically repeating earthquakes. Geophys. Res. Lett. 45, 699–707. https://doi.org/10.1002/2017GL075899.
McGuire, J.J., Boettcher, M.S., Jordan, T.H., 2005. Foreshock sequences and short-term earthquake predictability on East Pacific Rise transform faults. Nature 434, 457–461. https://doi.org/10.1038/nature03377.
McLaskey, G.C., 2019. Earthquake initiation from laboratory observations and implications for foreshocks. J. Geophys. Res. Solid Earth 124 (12). https://doi.org/10.1029/2019JB018363, 882–12,904.
McLaskey, G.C., Lockner, D.A., 2014. Preslip and cascade processes initiating laboratory stick slip. J. Geophys. Res. Solid Earth 119, 6323–6336. https://doi.org/10.1002/2014JB011220.
Meng, X., Peng, Z., 2014. Seismicity rate changes in the san jacinto fault zone and the salton Sea geothermal field following the 2010 Mw7.2 El Mayor-Cucapah earthquake. Geophys. J. Int. 197 (3), 1750–1762. https://doi.org/10.1093/gji/ggu085.
Meng, Q., Ni, S., Peng, Z., 2021. Complex source behaviors and spatio-temporal evolution of seismicity during the 2015-2016 earthquake sequence in Cushing. Oklahoma, J. Geophys. Res. 126, e2021JB022168. https://doi.org/10.1029/2021JB022168.
Meng, L., Huang, H., Bürgmann, R., Ampuero, J.P., Strader, A., 2015. Dual megathrust slip behaviors of the 2014 Iquique earthquake sequence. Earth Planet Sci. Lett. 411, 177–187. https://doi.org/10.1016/j.epsl.2014.11.041.
Mignan, A., 2014. The debate on the prognostic value of earthquake foreshocks: a meta-analysis. Sci. Rep. 4 (1), 4099. https://doi.org/10.1038/srep04099.
Mitchell, T.M., Faulkner, D.R., 2009. The nature and origin of off-fault damage surrounding strike-slip fault zones with a wide range of displacements: a field study from the Atacama fault system, northern Chile. J. Struct. Geol. 31 (8), 802–816. https://doi.org/10.1016/j.jsg.2009.05.002.
Mizrahi, L., Dallo, I., van der Elst, N.J., Christophersen, A., Spassiani, I., Werner, M.J., Iturrieta, P., Bayona, J.A., Iervolino, I., Schneider, M., Page, M.T., 2024. Developing, testing, and communicating earthquake forecasts: current practices and future

directions. Rev. Geophys. 62, e2023RG000823. https://doi.org/10.1029/2023RG000823.
Moein, M.J., Langenbruch, C., Schultz, R., Grigoli, F., Ellsworth, W.L., Wang, R., Rinaldi, A.P., Shapiro, S., 2023. The physical mechanisms of induced earthquakes. Nat. Rev. Earth Environ. 4 (12), 847–863. https://doi.org/10.1038/s43017-023-00497-8.
Mogi, K., 1963. Some discussions on aftershocks, foreshocks and earthquake swarms-the fracture of a semi finite body caused by an inner stress origin and its relation to the earthquake phenomena. Bull. Earthq. Res. Inst. 41, 615–658.
Mogi, K., 1985. Earthquake Prediction. Academic Press, Dordrecht.
Moore, J., McLennan, J., Allis, R., Pankow, K., Simmons, S., Podgorney, R., Wannamaker, P., Bartley, J., Jones, C., Rickard, W., 2019. The Utah Frontier Observatory for Research in Geothermal Energy (FORGE): an international laboratory for enhanced geothermal system technology development. In: 44th Workshop on Geothermal Reservoir Engineering. Stanford University, pp. 11–13.
Mousavi, S.M., Beroza, G.C., 2023. Machine learning in earthquake seismology. Annu. Rev. Earth Planet Sci. 51 (1), 105–129. https://doi.org/10.1146/annurev-earth-071822-100323.
Moutote, L., Marsan, D., Lengliné, O., Duputel, Z., 2021. Rare occurrences of non-cascading foreshock activity in Southern California. Geophys. Res. Lett. 48, e2020GL091757. https://doi.org/10.1029/2020GL091757.
Moutote, L., Itoh, Y., Lengliné, O., Duputel, Z., Socquet, A., 2023. Evidence of a transient aseismic slip driving the 2017 Valparaiso earthquake sequence, from foreshocks to aftershocks. J. Geophys. Res. Solid Earth 128, e2023JB026603. https://doi.org/10.1029/2023JB026603.
Münchmeyer, J., Leser, U., Tilmann, F., 2022. A probabilistic view on rupture predictability: all earthquakes evolve similarly. Geophys. Res. Lett. 49, e2022GL098344. https://doi.org/10.1029/2022GL098344.
Nadeau, R.M., McEvilly, T.V., 1999. Fault slip rates at depth from recurrence intervals of repeating microearthquakes. Science 285, 718–721. https://doi.org/10.1126/science.285.5428.718.
Nadeau, R.M., Guilhem, A., 2009. Nonvolcanic tremor evolution and the san simeon and Parkfield, California, earthquakes. science 325 (5937), 191–193. https://doi.org/10.1126/science.1174155.
Nakajima, J., 2022. Crustal structure beneath earthquake swarm in the Noto peninsula, Japan. 630 Earth Planets Space 74, 160. https://doi.org/10.1186/s40623-022-01719-x.
Nakajima, J., Hasegawa, A., 2023. Prevalence of repeating earthquakes in the continental crust and subducting slabs: triggering of earthquakes by aseismic slip. J. Geophys. Res. Solid Earth 128, e2022JB024667. https://doi.org/10.1029/2022JB024667.
Neves, M., Peng, Z., Lin, G., 2023. A high-resolution earthquake catalog for the 2004 M6 Parkfield earthquake sequence using a matched filter technique. Seismol Res. Lett. 94 (1), 507–521. https://doi.org/10.1785/0220220206.
Neves, M., Chuang, L.Y., Li, W., Peng, Z., Figueiredo, P.M., Ni, S., 2024. Complex rupture dynamics of the extremely shallow August 2020 M5. 1 Sparta, North Carolina earthquake. Communications Earth & Environment 5 (1), 163. https://doi.org/10.1038/s43247-024-01316-8.
Niu, F., Silver, P.G., Daley, T.M., Cheng, X., Majer, E.L., 2008. Preseismic velocity changes observed from active source monitoring at the Parkfield SAFOD drill site. Nature 454 (7201), 204–208. https://doi.org/10.1038/nature07111.
Ni, S., Wang, W., Li, L., 2010. The April 14th, 2010 Yushu earthquake, a devastating earthquake with foreshocks. Science China. Earth Sci. 53 (6), 791. https://doi.org/10.1007/s11430-010-0083-2.
Nishimura, T., Hiramatsu, Y., Ohta, Y., 2023. Episodic transient deformation revealed by the analysis of multiple GNSS networks in the Noto Peninsula, central Japan. Sci. Rep. 13, 8381. https://doi.org/10.1038/s41598-023-35459-z.
Noda, H., Nakatani, M., Hori, T., 2013. Large nucleation before large earthquakes is sometimes skipped due to cascade-up—implications from a rate and state simulation of faults with hierarchical asperities. J. Geophys. Res. Solid Earth 118, 2924–2952. https://doi.org/10.1002/jgrb.50211.
Ogata, Y., 1988. Statistical models for earthquake occurrences and residual analysis for point processes. J. Am. Stat. Assoc. 83, 9–27. https://doi.org/10.2307/2288914.
Ogata, Y., 2017. Statistics of earthquake activity: models and methods for earthquake predictability studies. Annu. Rev. Earth Planet Sci. 45 (1), 497–527. https://doi.org/10.1146/annurev-earth-063016-015918.
Ogata, Y., Utsu, T., Katsura, K., 1996. Statistical discrimination of foreshocks from other earthquake clusters. Geophys. J. Int. 127 (1), 17–30. https://doi.org/10.1111/j.1365-246X.1996.tb01531.x.
Ogata, Y., 2005. Detection of anomalous seismicity as a stress change sensor. J. Geophys. Res. Solid Earth 110 (B5). https://doi.org/10.1029/2004JB003245.
Ogata, Y., 2007. Seismicity and geodetic anomalies in a wide area preceding the Niigata-Ken-Chuetsu earthquake of 23 October 2004, central Japan. J. Geophys. Res. Solid Earth 112 (B10). https://doi.org/10.1029/2006JB004697.
Ohnaka, M., 1984. A sequence of seismic activity in the Kanto area precursory to the 1923 Kanto earthquake. Pure Appl. Geophys. 122, 848–862. https://doi.org/10.1007/BF00876388.
Ohnaka, M., 1992. Earthquake source nucleation: a physical model for short-term precursors. In: Mikumo, T., Aki, K., Ohnaka, M., Ruff, L.J., Spudich, P.K.P. (Eds.), Earthquake Source Physics and Earthquake Precursors, vol. 211, pp. 149–178. https://doi.org/10.1016/0040-1951(92)90057-D. Tectonophysics.
Ohnaka, M., 2013. The Physics of Rock Failure and Earthquakes. Cambridge University Press.
Ohnaka, M., Shen, L., 1999. Scaling of the shear rupture process from nucleation to dynamic propagation: Implications of geometric irregularity of the rupturing surfaces. J. Geophys. Res. 104 (B1), 817–844. https://doi.org/10.1029/1998JB900007.
Okubo, P.G., Dieterich, J.H., 1984. Effects of physical fault properties on frictional instabilities produced on simulated faults. J. Geophys. Res. 89 (B7), 5817–5827. https://doi.org/10.1029/jb089ib07p05817.
Omori, F., 1894. On the aftershocks of earthquakes. In: Journal of the College of Science, vol. 7. Imperial University of Tokyo, pp. 111–120.
Ostermeijer, G.A., Mitchell, T.M., Aben, F.M., Dorsey, M.T., Browning, J., Rockwell, T.K., Fletcher, J.M., Ostermeijer, F., 2020. Damage zone heterogeneity on seismogenic faults in crystalline rock; a field study of the Borrego Fault, Baja California. J. Struct. Geol. 137, 104016. https://doi.org/10.1016/j.jsg.2020.104016.
Ouzounov, D., Pulinets, S., Hattori, K., Taylor, P., 2018. Pre-earthquake Processes: a Multidisciplinary Approach to Earthquake Prediction Studies, vol. 234. John Wiley & Sons. https://doi.org/10.1002/9781119156949.
Ozacar, A.A., Beck, S.L., 2004. The 2002 Denali fault and 2001 Kunlun fault earthquakes: complex rupture processes of two large strike-slip events. Bull. Seismol. Soc. Am. 94 (6B), S278–S292. https://doi.org/10.1785/0120040604.
Papadopoulos, G.A., Agalos, A., Minadakis, G., Triantafyllou, I., Krassakis, P., 2020. Short-Term Foreshocks as Key Information for Mainshock Timing and Rupture: The Mw6.8 25 October 2018 Zakynthos Earthquake, Hellenic Subduction Zone. Sensors 20 (19), 5681. https://doi.org/10.3390/s20195681.
Peng, Z., Vidale, J.E., Marone, C., Rubin, A., 2005. Systematic variations in moment with recurrence interval of repeating aftershocks. Geophys. Res. Lett. 32 (15), L15301. https://doi.org/10.1029/2005GL022626.
Peng, Z., Zhao, P., 2009. Migration of early aftershocks following the 2004 Parkfield earthquake. Nature Geosci 2, 877–881. https://doi.org/10.1038/ngeo697.
Peng, Z., Gomberg, J., 2010. An integrated perspective of the continuum between earthquakes and slow-slip phenomena. Nat. Geosci. 3 (9), 599–607. https://doi.org/10.1038/ngeo940.
Peng, Z., Lei, X., Wang, Q.-Y., Wang, D., Mach, P., Yao, D., Kato, A., Obara, K., Campillo, M., 2025. The evolution process between the earthquake swarm beneath the Noto peninsula, Central Japan and the 2024 M 7.6 Noto hanto earthquake sequence. Earthquake Research Advances 5 (1), 100332. https://doi.org/10.1016/j.eqrea.2024.100332.
Perfettini, H., Frank, W.B., Marsan, D., Bouchon, M., 2018. A model of aftershock migration driven by afterslip. Geophys. Res. Lett. 45, 2283–2293. https://doi.org/10.1002/2017GL076287.
Petrillo, G., Kumazawa, T., Napolitano, F., Capuano, P., Zhuang, J., 2024. Fluids-triggered swarm sequence supported by a nonstationary epidemic-like description of seismicity. Seismol Res. Lett. 95 (6), 3207–3220. https://doi.org/10.1785/0220240056.
Picozzi, M., Iaccarino, A.G., Spallarossa, D., 2023. The preparatory process of the 2023 Mw 7.8 Türkiye earthquake. Sci. Rep. 13, 17853. https://doi.org/10.1038/s41598-023-45073-8.
Pritchard, M.E., Allen, R.M., Becker, T.W., Behn, M.D., Brodsky, E.E., Bürgmann, R., Ebinger, C., Freymueller, J.T., Gerstenberger, M., Haines, B., Kaneko, Y., 2020. New opportunities to study earthquake precursors. Seismological Society of America 91 (5), 2444–2447. https://doi.org/10.1785/0220200089.
Reasenberg, P.A., 1999. Foreshock occurrence before large earthquakes. J. Geophys. Res. 104 (B3), 4755–4768. https://doi.org/10.1029/1998JB900089.
Riggio, A., Santulin, M., 2015. Earthquake forecasting: a review of radon as seismic precursor. Bollettino Di Geofisica Teorica e Applicata 56 (2), 95–114. https://doi.org/10.4430/bgta0148.
Roeloffs, E.A., 2006. Evidence for aseismic deformation rate changes prior to earthquakes. Annu. Rev. Earth Planet Sci. 34 (1), 591–627. https://doi.org/10.1146/annurev.earth.34.031405.124947.
Ross, Z.E., Rollins, C., Cochran, E.S., Hauksson, E., Avouac, J.-P., Ben-Zion, Y., 2017. Aftershocks driven by afterslip and fluid pressure sweeping through a fault-fracture mesh. Geophys. Res. Lett. 44, 8260–8267. https://doi.org/10.1002/2017GL074634.
Ross, Z.E., Trugman, D.T., Hauksson, E., Shearer, P.M., 2019a. Searching for hidden earthquakes in Southern California. Science 364 (6442), 767–771. https://doi.org/10.1126/science.aaw6888.
Ross, Z.E., Idini, B., Jia, Z., Stephenson, O.L., Zhong, M., Wang, X., Zhan, Z., Simons, M., Fielding, E.J., Yun, S.H., Hauksson, E., 2019b. Hierarchical interlocked orthogonal faulting in the 2019 Ridgecrest earthquake sequence. Science 366 (6463), 346–351. https://doi.org/10.1126/science.aaz0109.
Ross, Z.E., Cochran, E.S., Trugman, D.T., Smith, J.D., 2020. 3D fault architecture controls the dynamism of earthquake swarms. Science 368 (6497), 1357–1361. https://doi.org/10.1126/science.abb0779.
Ruan, X., Meng, X., Peng, Z., Long, F., Xie, R., 2017. Microseismic activity in the last 5 months before the Mw7.9 Wenchuan earthquake. Bull. Seismol. Soc. Am. 107 (4), 1582–1592. https://doi.org/10.1785/0120160032.
Ruiz, S., Metois, M., Fuenzalida, A., Ruiz, J., Leyton, F., Grandin, R., Vigny, C., Madariaga, R., Campos, J., 2014. Intense foreshocks and a slow slip event preceded the 2014 Iquique Mw 8.1 earthquake. Science 345 (6201), 1165–1169. https://doi.org/10.1126/science.1256074.
Schoenball, M., Ellsworth, W.L., 2017. A systematic assessment of the spatio- temporal evolution of fault activation through induced seismicity in Oklahoma and southern Kansas. J. Geophys. Res. Solid Earth 122 (10). https://doi.org/10.1002/2017JB014850, 189–10,206.
Scholz, C.H., 2019. The Mechanics of Earthquakes and Faulting, 3rd ed. Cambridge Univ. Press, Cambridge, UK.
Scholz, C.H., Sykes, L.R., Aggarwal, Y.P., 1973. Earthquake prediction: a physical basis. Science 181, 803–810. https://doi.org/10.1126/science.181.4102.803.
Schurr, B., Asch, G., Hainzl, S., Bedford, J., Hoechner, A., Palo, M., Wang, R., Moreno, M., Bartsch, M., Zhang, Y., Oncken, O., 2014. Gradual unlocking of plate boundary controlled initiation of the 2014 Iquique earthquake. Nature 512 (7514), 299–302. https://doi.org/10.1038/nature13681.

Shapiro, S.A., Huenges, E., Borm, G., 1997. Estimating the crust permeability from fluid-injection-induced seismic emission at the KTB site. Geophys. J. Int. 131 (2), F15–F18. https://doi.org/10.1111/j.1365-246X.1997.tb01215.x.
Shearer, P.M., Meng, H., Fan, W., 2023. Earthquake detection using a nodal array on the San Jacinto fault in California: evidence for high foreshock rates preceding many events. J. Geophys. Res. Solid Earth 128, e2022JB025279. https://doi.org/10.1029/2022JB025279.
Shelly, D.R., 2009. Possible deep fault slip preceding the 2004 Parkfield earthquake, inferred from detailed observations of tectonic tremor. Geophys. Res. Lett. 36, L17318. https://doi.org/10.1029/2009GL039589.
Shelly, D.R., 2024. Examining the connections between earthquake swarms, crustal fluids, and large earthquakes in the context of the 2020–2024 Noto Peninsula, Japan, earthquake sequence. Geophys. Res. Lett. 51, e2023GL107897. https://doi.org/10.1029/2023GL107897.
Shelly, D., Beroza, G.C., Ide, S., 2007. Non-volcanic tremor and low-frequency earthquake swarms. Nature 446, 305–307. https://doi.org/10.1038/nature05666.
Shelly, D.R., Peng, Z., Hill, D.P., Aiken, C., 2011. Triggered creep as a possible mechanism for delayed dynamic triggering of tremor and earthquakes. Nature Geosci 4, 384–388. https://doi.org/10.1038/ngeo1141.
Shelly, D.R., Skoumal, R.J., Hardebeck, J.L., 2023. Fracture-mesh faulting in the swarm-like 2020 Maacama sequence revealed by high-precision earthquake detection, location, and focal mechanisms. Geophys. Res. Lett. 50, e2022GL101233. https://doi.org/10.1029/2022GL101233.
Sibson, R.H., 2007. An episode of fault-valve behaviour during compressional inversion? - the 2004 MJ6.8 Mid-Niigata Prefecture, Japan, earthquake sequence. Earth Planet Sci. Lett. 257 (1–2), 188–199. https://doi.org/10.1016/j.epsl.2007.02.031.
Silver, P.G., Wakita, H., 1996. A search for earthquake precursors. Science 273 (5271). https://doi.org/10.1126/science.273.5271.77, 77-77.
Sirorattanakul, K., Ross, Z.E., Khoshmanesh, M., Cochran, E.S., Acosta, M., Avouac, J.-P., 2022. The 2020 Westmorland, California earthquake swarm as aftershocks of a slow slip event sustained by fluid flow. J. Geophys. Res. Solid Earth 127, e2022JB024693. https://doi.org/10.1029/2022JB024693.
Socquet, A., Valdes, J.P., Jara, J., Cotton, F., Walpersdorf, A., Cotte, N., Specht, S., Ortega-Culaciati, F., Carrizo, D., Norabuena, E., 2017. An 8 month slow slip event triggers progressive nucleation of the 2014 Chile megathrust. Geophys. Res. Lett. 44, 4046–4053. https://doi.org/10.1002/2017GL073023.
Sornette, D., Ouillon, G., 2012. Dragon-kings: mechanisms, statistical methods and empirical evidence. Eur. Phys. J. Spec. Top. 205, 1–26. https://doi.org/10.1140/epjst/e2012-01559-5.
Sornette, D., Wei, X., Chen, X., 2024. Self-arresting earthquakes and critical sliding nucleation theory. https://doi.org/10.48550/arXiv.2402.14626.
Spassiani, I., Falcone, G., Murru, M., Marzocchi, W., 2023. Operational earthquake forecasting in Italy: validation after 10 yr of operativity. Geophys. J. Int. 234 (3), 2501–2518. https://doi.org/10.1093/gji/ggad256.
Stockman, S., Lawson, D.J., Werner, M.J., 2023. Forecasting the 2016–2017 Central Apennines earthquake sequence with a neural point process. Earth's Future 11, e2023EF003777. https://doi.org/10.1029/2023EF003777.
Stein, R.S., Bird, P., 2024. Why do great continental transform earthquakes nucleate on branch faults? Seismol Res. Lett. 95 (6), 3406–3415. https://doi.org/10.1785/0220240175.
Sugan, M., Kato, A., Miyake, H., Nakagawa, S., Vuan, A., 2014. The preparatory phase of the 2009 Mw 6.3 L'Aquila earthquake by improving the detection capability of low-magnitude foreshocks. Geophys. Res. Lett. 41 (17), 6137–6144. https://doi.org/10.1002/2014GL061199.
Sugan, M., Campanella, S., Vuan, A., Shakibay Senobari, N., 2022. A Python code for detecting true repeating earthquakes from self-similar waveforms (FINDRES). Seismological Res. Lett. 93 (5), 2847–2857. https://doi.org/10.1785/0220220048.
Sugan, M., Campanella, S., Chiaraluce, L., Michele, M., Vuan, A., 2023. The unlocking process leading to the 2016 Central Italy seismic sequence. Geophys. Res. Lett. 50, e2022GL101838. https://doi.org/10.1029/2022GL101838.
Suyehiro, S., Sekiya, H., 1972. Foreshocks and earthquake prediction. Tectonophysics 14 (3–4), 219–225. https://doi.org/10.1016/0040-1951(72)90070-4.
Tan, Y.J., Waldhauser, F., Ellsworth, W.L., Zhang, M., Zhu, W., Michele, M., Chiaraluce, L., Beroza, G.C., Segou, M., 2021. Machine-learning-based high-resolution earthquake catalog reveals how complex fault structures were activated during the 2016-2017 central Italy sequence. The Seismic Record 1 (1), 11–19. https://doi.org/10.1785/0320210001.
Toda, S., Stein, R.S., 2024. Intense seismic swarm punctuated by a magnitude 7.5 Japan shock. Temblor. https://doi.org/10.32858/temblor.333.
Toda, S., Stein, R.S., Sevilgen, V., 2024. Japan's magnitude 7.1 shock triggers megaquake warning. How likely is this scenario? Temblor. https://doi.org/10.32858/temblor.348.
Trugman, D.T., Ross, Z.E., 2019. Pervasive foreshock activity across southern California. Geophys. Res. Lett. 46, 8772–8781. https://doi.org/10.1029/2019GL083725.
Twardzik, C., Duputel, Z., Jolivet, R., Klein, E., Rebischung, P., 2022. Bayesian inference on the initiation phase of the 2014 Iquique, Chile, earthquake. Earth Planet Sci. Lett. 600, 117835. https://doi.org/10.1016/j.epsl.2022.117835.
Uchida, N., 2019. Detection of repeating earthquakes and their application in characterizing slow fault slip. Prog. Earth Planet. Sci. 6 (1), 1–21. https://doi.org/10.1186/s40645-019-0284-z.
Uchida, N., Bürgmann, R., 2019. Repeating earthquakes. Annu. Rev. Earth Planet Sci. 47 (1), 305–332. https://doi.org/10.1146/annurev-earth-053018-060119.
Umeda, K., Yamazaki, Y., Sumino, H., 2024. Geochemical signature of deep fluids triggering earthquake swarm in the Noto Peninsula, central Japan. Geophys. Res. Lett. 51, e2024GL108581. https://doi.org/10.1029/2024GL108581.
Unsworth, M., Rondenay, S., 2013. Mapping the distribution of fluids in the crust and lithospheric mantle utilizing geophysical methods. In: Metasomatism and the Chemical Transformation of Rock. Lecture Notes in Earth System Sciences. Springer, Berlin, Heidelberg. https://doi.org/10.1007/978-3-642-28394-9_13.
Utsu, T., Ogata, Y., Matsu'ura, R.S., 1995. The centenary of the Omori formula for a decay law of aftershock activity. J. Phys. Earth 43 (1), 1–33. https://doi.org/10.4294/jpe1952.43.1.
Utsu, T., 2002. Statistical features of seismicity. In: Lee, William H.K., Kanamori, Hiroo, Jennings, Paul C., Kisslinger, Carl (Eds.), International Geophysics, Academic Press, vol. 81, pp. 719–732. https://doi.org/10.1016/S0074-6142(02)80246-7.
Uyeda, S., Nagao, T., Kamogawa, M., 2009. Short-term earthquake prediction: current status of seismo-electromagnetics. Tectonophysics 470 (3–4), 205–213. https://doi.org/10.1016/j.tecto.2008.07.019.
Valoroso, L., Chiaraluce, L., Piccinini, D., Di Stefano, R., Schaff, D., Waldhauser, F., 2013. Radiography of a normal fault system by 64,000 high-precision earthquake locations: the 2009 L'Aquila (central Italy) case study. J. Geophys. Res. Solid Earth 118, 1156–1176. https://doi.org/10.1002/jgrb.50130.
van den Ende, M.P.A., Ampuero, J.-P., 2020. On the statistical significance of foreshock sequences in Southern California. Geophys. Res. Lett. 47, e2019GL086224. https://doi.org/10.1029/2019GL086224.
van der Elst, 2021. B-positive: A robust estimator of aftershock magnitude distribution in transiently incomplete catalogs. J. Geophys. Res. Solid Earth 126, e2020JB021027. https://doi.org/10.1029/2020JB021027.
Vidale, J.E., Ellsworth, W.L., Cole, A., Marone, C., 1994. Variations in rupture process with recurrence interval in a repeated small earthquake. Nature 368, 624–626. https://doi.org/10.1038/368624a0, 1994.
Vidale, J.E., Shearer, P.M., 2006. A survey of 71 earthquake bursts across southern California: exploring the role of pore fluid pressure fluctuations and aseismic slip as drivers. J. Geophys. Res. Solid Earth 111 (B5). https://doi.org/10.1029/2005JB004034.
Volpe, G., Pozzi, G., Collettini, C., Spagnuolo, E., Achtziger-Zupančič, P., Zappone, A., Aldega, L., Meier, M.A., Giardini, D., Cocco, M., 2023. Laboratory simulation of fault reactivation by fluid injection and implications for induced seismicity at the BedrettoLab, Swiss Alps. Tectonophysics 862, 229987. https://doi.org/10.1016/j.tecto.2023.229987.
Vuan, A., Sugan, M., Amati, G., Kato, A., 2018. Improving the detection of low-magnitude seismicity preceding the Mw 6.3 L'Aquila earthquake: development of a scalable code based on the cross correlation of template earthquakes. Bull. Seismol. Soc. Am. 108 (1), 471–480.doi. https://doi.org/10.1785/0120170106.
Walter, J.I., Meng, X., Peng, Z., Schwartz, S.Y., Newman, A.V., Protti, M., 2015. Far-field triggering of foreshocks near the nucleation zone of the 5 September 2012 (MW 7.6) Nicoya Peninsula, Costa Rica earthquake. Earth Planet Sci. Lett. 431, 75–86. https://doi.org/10.1016/j.epsl.2015.09.017.
Wang, H., Fu, T., Du, Y., Gao, W., Huang, K., Liu, Z., Chandak, P., Liu, S., Van Katwyk, P., Deac, A., Anandkumar, A., 2023. Scientific discovery in the age of artificial intelligence. Nature 620 (7972), 47–60. https://doi.org/10.1038/s41586-023-06221-2.
Wang, K., Chen, Q.F., Sun, S., Wang, A., 2006. Predicting the 1975 Haicheng earthquake. Bull. Seismol. Soc. Am. 96 (3), 757–795. https://doi.org/10.1785/0120050191.
Wang, K., Rogers, G.C., 2014. Earthquake preparedness should not fluctuate on a daily or weekly basis. Seismol Res. Lett. 85, 569–571. https://doi.org/10.1785/0220130195.
Wang, K., Rogers, G.C., 2017. Beating fear with hope: on sustaining earthquake preparedness. Seismol Res. Lett. 88 (1), 171–176. https://doi.org/10.1785/0220160106.
Wang, K., Dreger, D.S., Tinti, E., Bürgmann, R., Taira, T.A., 2020. Rupture process of the 2019 Ridgecrest, California Mw 6.4 foreshock and Mw 7.1 earthquake constrained by seismic and geodetic data. Bull. Seismol. Soc. Am. 110 (4), 1603–1626. https://doi.org/10.1785/0120200108.
Wang, K., Peng, Z., Liang, S., Luo, J., Zhang, K., He, C., 2024a. Migrating foreshocks driven by a slow slip event before the 2021 MW 6.1 Yangbi, China earthquake. J. Geophys. Res. Solid Earth 129, e2023JB027209. https://doi.org/10.1029/2023JB027209.
Wang, Q.Y., Cui, X., Frank, W.B., Lu, Y., Hirose, T., Obara, K., 2024b. Untangling the environmental and tectonic drivers of the Noto earthquake swarm in Japan. Sci. Adv. 10 (19), eado1469. https://doi.org/10.1126/sciadv.ado1469.
Wang, L., Xu, S., Zhuo, Y., Liu, P., Ma, S., 2024c. Unraveling the roles of fault asperities over earthquake cycles. Earth Planet Sci. Lett. 636, 118711. https://doi.org/10.1016/j.epsl.2024.118711.
Wang, W., Shearer, P.M., Vidale, J.E., Xu, X., Trugman, D.T., Fialko, Y., 2022. Tidal modulation of seismicity at the Coso geothermal field. Earth Planet Sci. Lett. 579, 117335. https://doi.org/10.1016/j.epsl.2021.117335.
Wei, X., Liu, Y., Xu, J., Liu, W., Chen, X., 2024. A detailed understanding of slow self-arresting rupture. J. Geophys. Res. Solid Earth 129, e2024JB028881. https://doi.org/10.1029/2024JB028881.
Wetzler, N., Lay, T., Brodsky, E.E., 2023. Global characteristics of observable foreshocks for large earthquakes. Seismol Res. Lett. 94 (5), 2313–2325. https://doi.org/10.1785/0220220397.
Wickham-Piotrowski, A., Font, Y., Regnier, M., Delouis, B., Nocquet, J.M., De Barros, L., Durand, V., Bletery, Q., Segovia, M., 2024. Intraslab seismicity migration simultaneously with an interface slow slip event along the Ecuadorian subduction zone. Tectonophysics 883, 230365. https://doi.org/10.1016/j.tecto.2024.230365.
Wu, B.S., McLaskey, G.C., 2022. Testing Earthquake Nucleation Length Scale with Pawnee Aftershocks. Seismol. Res. Lett. 93, 2147–2160. https://doi.org/10.1785/0220210184.
Wu, J., Yao, D., Meng, X., Peng, Z., Su, J., Long, F., 2017. Spatial-temporal evolutions of early aftershocks following the 2013 Mw 6.6 Lushan earthquake in Sichuan, China.

J. Geophys. Res. Solid Earth 122, 2873–2889. https://doi.org/10.1002/2016JB013706.
Xu, D., Li, Z., Zhang, Z., Yu, H., Xu, J., Yang, Z., Chen, X., 2024a. The 2022 Mw 6.6 Menyuan earthquake: an early-terminated runaway rupture by the complex fault geometry. Earth Planet Sci. Lett. 638, 118746. https://doi.org/10.1016/j.epsl.2024.118746.
Xu, J., Zhang, H., Chen, X., 2015. Rupture phase diagrams for a planar fault in 3-D full-space and half-space. Geophys. J. Int. 202 (3), 2194–2206. https://doi.org/10.1093/gji/ggv284.
Xu, L., Ji, C., Meng, L., Ampuero, J.P., Yunjun, Z., Mohanna, S., Aoki, Y., 2024b. Dual-initiation ruptures in the 2024 Noto earthquake encircling a fault asperity at a swarm edge. Science 385 (6711), 871–876. https://doi.org/10.1126/science.adp0493.
Yagi, Y., Okuwaki, R., Enescu, B., Hirano, S., Yamagami, Y., Endo, S., Komoro, T., 2014. Rupture process of the 2014 Iquique Chile earth- quake in relation with the foreshock activity. Geophys. Res. Lett. 41 (12), 4201–4206. https://doi.org/10.1002/2014gl060274.
Yamashita, F., Fukuyama, E., Xu, S., Kawakata, H., Mizoguchi, K., Takizawa, S., 2021. Two end-member earthquake preparations illuminated by foreshock activity on a meter-scale laboratory fault. Nature Communication 12 (1), 4302. https://doi.org/10.1038/s41467-021-24625-4.
Yamashita, F., Fukuyama, E., Xu, S., 2022. Foreshock activity promoted by locally elevated loading rate on a 4-m-long laboratory fault. J. Geophys. Res. Solid Earth 127, e2021JB023336. https://doi.org/10.1029/2021JB023336.
Yao, D., Walter, J.I., Meng, X., Hobbs, T.E., Peng, Z., Newman, A.V., Schwartz, S.Y., Protti, M., 2017. Detailed spatio-temporal evolution of microseismicity and repeating earthquakes following the 2012 Mw 7.6 Nicoya earthquake. J. Geophys. Res. 122. https://doi.org/10.1002/2016JB013632.
Yao, D., Huang, Y., Peng, Z., Castro, R.R., 2020. Detailed investigation of the foreshock sequence of the 2010 Mw 7.2 El Mayor-Cucapah earthquake. J. Geophys. Res. 124 (6), e2019JB019076. https://doi.org/10.1029/2019JB019076.
Yoshida, K., Uno, M., Matsuzawa, T., Yukutake, Y., Mukuhira, Y., Sato, H., Yoshida, T., 2023a. Upward earthquake swarm migration in the northeastern Noto Peninsula, Japan, initiated from a deep ring-shaped cluster: possibility of fluid leakage from a hidden magma system. J. Geophys. Res. Solid Earth 128, e2022JB026047. https://doi.org/10.1029/2022JB026047.
Yoshida, K., Uchida, N., Matsumoto, Y., Orimo, M., Okada, T., Hirahara, S., Kimura, S., Hino, R., 2023b. Updip fluid flow in the crust of the northeastern Noto Peninsula, Japan, triggered the 2023 Mw 6.2 Suzu earthquake during swarm activity. Geophys. Res. Lett. 50, e2023GL106023. https://doi.org/10.1029/2023GL106023.
Yoshida, K., Takagi, R., Fukushima, Y., Ando, R., Ohta, Y., Hiramatsu, Y., 2024. Role of a hidden fault in the early process of the 2024 Mw7.5 Noto Peninsula earthquake. Geophys. Res. Lett. 51, e2024GL110993. https://doi.org/10.1029/2024GL110993.
Yu, H., Liu, J., Ma, Y., Yan, R., Yu, C., Li, S., Yang, Z., Hong, M., Tu, H., Zhang, Z., 2022. A possible characteristic of foreshocks derived from the evaluation of loading/unloading induced by earth tides. Front. Earth Sci. 1375. https://doi.org/10.3389/feart.2022.967264.
Yue, H., Ross, Z.E., Liang, C., Michel, S., Fattahi, H., Fielding, E., Moore, A., Liu, Z., Jia, B., 2017. The 2016 Kumamoto Mw= 7.0 earthquake: a significant event in a fault–volcano system. J. Geophys. Res. Solid Earth 122 (11), 9166–9183. https://doi.org/10.1002/2017JB014525.
Yue, H., Sun, J., Wang, M., Shen, Z., Li, M., Xue, L., Lu, W., Zhou, Y., Ren, C., Lay, T., 2021. The 2019 Ridgecrest, California earthquake sequence: evolution of seismic and aseismic slip on an orthogonal fault system. Earth Planet Sci. Lett. 570, 117066. https://doi.org/10.1016/j.epsl.2021.117066.
Zaccagnino, D., Vallianatos, F., Michas, G., Telesca, L., Doglioni, C., 2024. Are foreshocks fore-shocks? J. Geophys. Res. Solid Earth 129, e2023JB027337. https://doi.org/10.1029/2023JB027337.
Zhai, Q., Peng, Z., Chuang, L.Y., Wu, Y.-M., Hsu, Y.-J., Wdowinski, S., 2021. Investigating the impacts of a wet typhoon on microseismicity: a case study of the 2009 typhoon morakot in taiwan based on a template matching catalog. J. Geophys. Res. Solid Earth 126 (12). https://doi.org/10.1029/2021jb023026.
Zhai, Q., Zhan, Z., Chavarria, J.A., 2024. Thousand-kilometer DAS array reveals an uncatalogued magnitude-5 dynamically triggered event after the 2023 Turkey earthquake. J. Geophys. Res. Solid Earth 129 (3), e2023JB027680. https://doi.org/10.1029/2023JB027680.
Zhan, Z., 2020. Distributed acoustic sensing turns fiber-optic cables into sensitive seismic antennas. Seismol Res. Lett. 91 (1), 1–15. https://doi.org/10.1785/0220190112.
Zhang, M., Wen, L., 2015. An effective method for small event detection: match and locate (M&L). Geophys. J. Int. 200 (3), 1523–1537. https://doi.org/10.1093/gji/ggu466.
Zhao, P., Peng, Z., 2009. Depth extent of damage zones around the central Calaveras fault from waveform analysis of repeating earthquakes. Geophys. J. Int. 179, 1817–1830. https://doi.org/10.1111/j.1365-246X.2009.04385.x.
Zhao, Y., Jiang, G., Lei, X., Xu, C., Zhao, B., Qiao, X., 2023. The 2021 Ms 6.0 luxian (China) earthquake: blind reverse-fault rupture in deep sedimentary formations likely induced by pressure perturbation from hydraulic fracturing. Geophys. Res. Lett. 50, 1–12. https://doi.org/10.1029/2023GL103209.
Zhou, Y., Ren, C., Ghosh, A., Meng, H., Fang, L., Yue, H., Zhou, S., Su, Y., 2022. Seismological characterization of the 2021 Yangbi foreshock-mainshock sequence, Yunnan, China: more than a triggered cascade. J. Geophys. Res. Solid Earth 127 (8), e2022JB024534. https://doi.org/10.1029/2022JB024534.
Zhu, G., Yang, H., Tan, Y.J., Jin, M., Li, X., Yang, W., 2022a. The cascading foreshock sequence of the Ms 6.4 Yangbi earthquake in Yunnan, China. Earth Planet Sci. Lett. 591, 591117594. https://doi.org/10.1016/j.epsl.2022.117594.
Zhu, J.B., Kang, J.Q., Elsworth, D., Xie, H.P., Ju, Y., Zhao, J., 2021. Controlling induced earthquake magnitude by cycled fluid injection. Geophys. Res. Lett. 48, e2021GL092885. https://doi.org/10.1029/2021GL092885.
Zhu, S., Li, S., Peng, Z., Xie, Y., 2022b. Imitation learning of neural spatio-temporal point processes. IEEE Trans. Knowl. Data Eng. 34 (11), 5391–5402. https://doi.org/10.1109/TKDE.2021.3054787.
Zlydenko, O., Elidan, G., Hassidim, A., Kuklиansky, D., Matias, Y., Meade, B., Molchanov, A., Nevo, S., Bar-Sinai, Y., 2023. A neural encoder for earthquake rate forecasting. Sci. Rep. 13 (1), 12350. https://doi.org/10.1038/s41598-023-38033-9.
Zuo, Z.R., Zhang, G.M., Wu, J.P., 1996. Analysis of the 1976 Longling, Yunnan, earthquake sequence of Ms 7.4. Chin. J. Geophys. 39 (5), 653–659 (In Chinese). http://www.geophy.cn/article/id/cjg_4098.